

A Bayesian Approach to Directed Acyclic Graphs with a Candidate Graph

Evan A Martin*

The Graduate Program in Bioinformatics and Computational Biology, University
of Idaho

and

Audrey Qiuyan Fu

Department of Statistical Science, University of Idaho

June 19, 2022

Abstract

Directed acyclic graphs represent the dependence structure among multiple variables. When learning these graphs from data, different amounts of information may be available for different edges. Although many methods have been developed to learn the topology of these graphs, most of these methods do not provide a measure of the uncertainty in the inference. Here, we propose a Bayesian method, namely baycn (BAYesian Causal Network), to estimate the posterior probability of three states for each inferred edge: present with one direction ($X \rightarrow Y$), present with the opposite direction ($X \leftarrow Y$), and absent. Unlike existing Bayesian methods, our method requires that the prior probabilities of the three states be specified, and therefore provides a coherent interpretation of the posterior probabilities. We develop a fast Metropolis-Hastings Markov chain Monte Carlo algorithm for the inference. To perform the inference efficiently, our algorithm takes as input a candidate graph, which may be the output of another graph inference method and may contain false edges. In simulation studies our method achieves high accuracy with small variation across different scenarios and is comparable or better than existing Bayesian methods.

Keywords: Bayesian inference, causal inference, directed acyclic graph, Markov chain Monte Carlo

**This work was supported by the NIH/NHGRI grant R00HG007368 (to AQF); and partially by the NIH/NIGMS grant P20GM104420 to the Center for Modeling Complex Interactions at the University of Idaho.*

1 Introduction

Directed acyclic graphs (DAGs) represent the dependence structure among multiple variables and are used in a wide range of fields and applications (Korb and Nicholson, 2010). Directed edges may be interpreted as causal relationships: for example, the edge $X \rightarrow Y$ in a graph can be interpreted as X being causal to Y (under assumptions that may be specific to the scientific problem). It has been of great interest to learn the structure of the DAG, such that we can understand the relationships among the variables. On the other hand, data often contain different amounts of information for different edges. Just because two edges (e.g., $X \rightarrow Y$ and $X \rightarrow Z$) are inferred to be in the DAG, it does not mean that the two edges are necessarily supported by equally strong evidence. It is therefore of interest to also quantify the level of uncertainty in the inferred graph, preferably for each individual edge.

Many methods have been developed to infer DAGs and largely fall into three main classes (Koller and Friedman, 2009): the constraint-based methods, the score-based learning methods, and the hybrid methods. Constraint-based methods start with a fully connected graph, conduct a series of marginal and conditional independence tests among pairs of nodes, and remove the edge if the test does not reject the null hypothesis of independence between the two nodes (Scutari, 2009; Colombo and Maathuis, 2014). A major benefit of these algorithms is their efficiency and scalability to large graphs. On the other hand, these algorithms typically do not adjust for multiple testing and can be sensitive to how nodes (i.e., variables) are ordered (Colombo and Maathuis, 2014; Badsha and Fu, 2019).

Score-based learning methods move through the graph space according to a score computed for the graph given the data. Non-Bayesian methods may take a hill climbing (Russell and Norvig, 2009; Margaritis, 2003) approach to maximize the score, which is typically based on likelihood or penalized likelihood. Bayesian methods sample directly from a closed-form posterior distribution (Schwaller et al., 2015; Leday and Richardson, 2018) or, more often, use a Markov Chain Monte Carlo (MCMC) algorithm (Friedman and Koller, 2003; Giudici and Castelo, 2003; Goudie and Mukherjee, 2016; Grzegorzczak and Husmeier, 2008; He et al., 2013; Kuipers and Moffa, 2017; Kuipers et al., 2018; Madigan et al., 1995; Mohammadi et al., 2015) for inference, moving through graph space by proposing new graph structures, scoring them, and determining whether to stay at the current structure or move to the proposed structure.

The score-based Bayesian MCMC methods vary in how they move around in graph space but each of them calculates the posterior probability of the graph. They can be further broken down into two different classes the structure-based algorithms and the order-based algorithms. The structure-based algorithms search the space of DAGs (Madigan et al., 1995; Goudie and Mukherjee, 2016), considering different combinations of edges and edge directions, and sampling the DAGs based on the posterior distribution. The order-based algorithms search the space of node orderings (Friedman and Koller, 2003; Kuipers et al., 2018). These methods require that a parent node must appear after the child node in the node ordering. The space of node orderings is much smaller than the graph space because one ordering can represent multiple DAGs. However, this method may introduce bias into the inference when certain DAGs are over represented. Kuipers and Moffa (Kuipers and Moffa, 2017) proposed a variation based on the order of node partitions, which are more succinct representations of a DAG than node orderings. A partition divides the nodes into subsets and can group multiple node orderings of the same DAG into one partition.

Hybrid methods have been proposed to combine the strengths of the constraint- and scored-based approaches. For example, a non-Bayesian hybrid method is the max-min hill-climbing algorithm (Tsamardinos et al., 2006). It first applies the PC algorithm (named after developers Peter

Spirtes and Clark Glymour) (Spirtes et al., 2000; Kalisch et al., 2012) to infer a candidate graph, and then performs a greedy hill-climbing search for graphs similar to the candidate graph. Bayesian hybrid methods have also been proposed to address the speed issue of the MCMC methods.

In summary, Bayesian methods for DAGs have the advantage of quantifying the uncertainty in the inference, although they are typically unable to deal with larger graphs or are not as fast as non-Bayesian methods. Here, we propose a novel Bayesian approach, namely baycn (BAYesian Causal Network), for inferring a DAG. Our method also defines three states for an edge, namely present with one direction ($X \rightarrow Y$), present with the opposite direction ($X \leftarrow Y$), and absent. We specify the prior probabilities of these states and estimate their posterior probabilities. Whether the posterior probability for an edge state is large enough depends on the corresponding prior. In other words, if the data are informative about an edge, then the posterior probabilities of this edge should be substantially different from the prior. For example, if the prior probability is 0.05 for an edge state, then a posterior probability of 0.3 indicates support from the data for this state, even though 0.3 is not typically considered a large posterior. We develop a Metropolis-Hastings MCMC algorithm that samples the space of edge states. It removes directed cycles when moving between graphs, and accounts for Markov equivalence, which refers to different DAGs having the same likelihood. Our method can be used either as a hybrid or as a stand-alone score-based method. As a hybrid method, we can use the graph inferred by other more efficient graph inference methods as input; the input graph may contain false edges or undirected edges but can help reduce the search space to a more manageable size. We perform simulation to examine the performance of our method, and compare with other Bayesian methods for DAGs.

2 Model

2.1 The Bayesian graphical model

A graph $\mathcal{G} = (\mathbf{V}, \mathbf{E})$ is a set of vertices (nodes) $\mathbf{V} = \{1, 2, \dots, b\}$ and edges $\mathbf{E} \subseteq \mathbf{V} \times \mathbf{V}$, where $\mathbf{V} \times \mathbf{V}$ is the set of all ordered pairs of nodes, such as (j, k) , which denotes an edge pointing from node j to node k where $j, k \in \mathbf{V}$. The structure (or topology) of the graph is typically represented by the adjacency matrix \mathbf{A} of dimension $b \times b$: $A_{jk} = 1$ and $A_{kj} = 0$ represent an edge from node j to node k , and $A_{jk} = 0$ and $A_{kj} = 1$ represent an edge from node k to node j . If $A_{jk} = A_{kj} = 0$ there is no edge between nodes j and k .

We introduce an alternate representation of the graph to directly describe the states of individual edges with the vector $\mathbf{S} = (S_1, S_2, \dots, S_m)$, where m is the number of edges. Each edge is in one of three possible states:

$$S_i = \begin{cases} 0, & \text{if } A_{jk} = 1 \text{ and } A_{kj} = 0 \text{ where } j < k; \\ 1, & \text{if } A_{kj} = 1 \text{ and } A_{jk} = 0 \text{ where } j < k; \\ 2, & \text{if } A_{jk} = A_{kj} = 0, \end{cases}$$

such that

$$\sum_{k=0}^2 \Pr(S_i = k) \equiv p_k = 1. \quad (1)$$

Note that the state 2 represents the absence of the edge. With a slight abuse of notation, we draw

connections to the adjacency matrix and define

$$\Pr(S_{jk} = 0) \equiv \Pr(A_{jk} = 1) \text{ and } \Pr(S_{jk} = 1) \equiv \Pr(A_{kj} = 1), \quad (2)$$

where S_{jk} with the double subscript represents the state of the edge between nodes j and k . Under this notation,

$$\Pr(S_{jk} = 2) = 1 - \Pr(A_{jk} = 1) - \Pr(A_{kj} = 1). \quad (3)$$

Incidentally, if $\Pr(S_i = 0) = \Pr(S_i = 1) = 0.5$, then the i th edge is bidirected with the two directions being equally likely.

When data are available at all the nodes, the set of nodes \mathbf{V} corresponds to a random vector $\mathbf{T} = (T_1, T_2, \dots, T_b)^T$. We aim to infer the posterior edge state probability $\Pr(S_i | \mathbf{T})$ for all edges. Similar to Equation (1), the posterior probabilities of the three states for an edge also add up to 1. If $\Pr(S_i = 2 | \mathbf{T}) > 0.5$, then the data do not support the presence of this edge; in other words, this is a false edge. Alternatively, if $\Pr(S_i = 0 | \mathbf{T}) = \Pr(S_i = 1 | \mathbf{T}) = 0.4$, the data support the presence of this edge but there is not enough information to determine the direction.

The probability of the graph can be written as a product of conditional probabilities where each node is conditioned on its parents

$$\Pr(\mathbf{T} | \mathbf{S}, \boldsymbol{\theta}) = \prod_{j=1}^b \Pr(T_j | pa(T_j), \boldsymbol{\theta}_j) \quad (4)$$

where $pa(T_j)$ are the parents of T_j , $\boldsymbol{\theta}_j$ is the parameter vector for the distribution of T_j , and $\boldsymbol{\theta} = \{\boldsymbol{\theta}_1, \dots, \boldsymbol{\theta}_b\}$. If $pa(T_j) = \emptyset$ the probability is reduced to a marginal probability $\Pr(T_j | \boldsymbol{\theta}_j)$.

We assume normality for the data at each node:

$$T_j \sim \mathbf{N}(\mu_j, \sigma_j^2), \quad (5)$$

$$\mu_j = \beta_0 + \sum_{k \in pa(T_j)} \beta_k T_k, \quad (6)$$

where μ_j is the mean and σ_j^2 the variance. If the node T_j does not have any parents then $\mu_j = \beta_0$.

2.2 Markov Equivalence

Two graphs are Markov equivalent if they have the same likelihood (Verma and Pearl, 1990). A set of Markov equivalent graphs form a Markov equivalence class. For example, the graphs $T_1 \rightarrow T_2 \rightarrow T_3$, $T_1 \leftarrow T_2 \rightarrow T_3$, and $T_1 \leftarrow T_2 \leftarrow T_3$ are Markov equivalent and all represent marginal dependence between T_1 and T_3 (i.e., $T_1 \not\perp T_3$) and conditional independence given T_2 (i.e., $T_1 \perp T_3 | T_2$). By contrast, the graph $T_1 \rightarrow T_2 \leftarrow T_3$, also known as a v structure, has no Markov equivalent graphs. In this graph T_1 and T_3 are marginally independent (i.e., $T_1 \perp T_3$) and conditionally dependent given T_2 (i.e., $T_1 \not\perp T_3 | T_2$). The probability of the edge states for each edge in a graph need to account for Markov equivalence (see examples in Figure 1).

2.3 The Metropolis-Hastings MCMC Algorithm

We have developed a Metropolis-Hastings algorithm that proposes changes to edge states. The input is the binary adjacency matrix of a candidate graph and the data at the nodes. The candidate

graph may be a fully connected graph, where all nodes are connected. A more efficient approach is to run a fast graph inference algorithm to produce a candidate graph and use it as the input, even if this graph may contain false edges. We will use the graph skeleton as the candidate graph, where the edges are undirected, and the adjacency matrix is therefore symmetric.

At the t th iteration, the key steps of the Metropolis-Hastings algorithm are:

1. Generate a proposal graph $\mathbf{S}'_{(t)}$ from the current graph $\mathbf{S}_{(t-1)}$. When $t = 1$, the current graph is randomly generated from the candidate graph in the input.
2. Check for and remove directed cycles in $\mathbf{S}'_{(t)}$.
3. Calculate the acceptance probability $\alpha_{(t)}$

$$\alpha_{(t)} = \min \left\{ \frac{\Pr(\mathbf{S}'_{(t)}) \Pr(\mathbf{T} | \mathbf{S}'_{(t)}, \boldsymbol{\theta}_{(t)}) \Pr(\mathbf{S}_{(t-1)} | \mathbf{S}'_{(t)})}{\Pr(\mathbf{S}_{(t-1)}) \Pr(\mathbf{T} | \mathbf{S}_{(t-1)}, \boldsymbol{\theta}_{(t-1)}) \Pr(\mathbf{S}'_{(t)} | \mathbf{S}_{(t-1)})}, 1 \right\}, \quad (7)$$

where $\Pr(\mathbf{S})$ is the prior probability of the graph, $\Pr(\mathbf{T} | \mathbf{S}, \boldsymbol{\theta})$ the graph likelihood, and $\Pr(\mathbf{S} | \mathbf{S}')$ the transition probability.

4. Generate a random probability u from the uniform distribution $U(0, 1)$.

Accept the proposal and set $\mathbf{S}_{(t)} = \mathbf{S}'_{(t)}$ if $u < \alpha_{(t)}$; or stay at the current graph and set $\mathbf{S}_{(t)} = \mathbf{S}_{(t-1)}$ otherwise.

To generate the proposal graph in step 1, we first determine the number of edges to change states by sampling from a binomial distribution $B(m, 1/m)$, where m is the number of edges in the network and $1/m$ is the “success” probability. For each of the selected edges, we then sample from a Bernoulli distribution with probability p to decide which edge state to change to. Since we do not allow for the edge to remain at the same state, p is determined by that of the other two possible edge states. For example, if an edge in state 0 is selected to change states, and if the prior probability for the three edge states are $p_0 = 0.05$, $p_1 = 0.05$, and $p_2 = 0.9$, then the probability of switching to state 1 is $p = 0.05/(0.05 + 0.9)$.

This MCMC algorithm generates a sample of graphs represented by edge states. For each edge, the relative frequencies of the three states in the MCMC sample provide an estimate of the posterior probabilities of edge states $\Pr(S_i | \mathbf{T})$.

Through changes in edge states, our algorithm can sample from multiple Markov equivalent graphs and thus produce posterior probabilities that account for Markov equivalence. With sufficient data, the posterior probabilities of edge states should be the same asymptotically as expected under Markov equivalence.

2.4 Identifying and removing directed cycles

In a directed cycle, one can follow the directed edges and return to the starting node (e.g., $T_1 \rightarrow T_2 \rightarrow T_3 \rightarrow T_1$). Directed cycles can have a higher likelihood than the true graph, a graph with directed edges but no cycles, and therefore should be removed during the MCMC iterations when generating a proposal graph.

We have developed a “cycle finder” algorithm (Supplementary Section S1) to find all directed cycles (including overlapping cycles, as well as multiple disjoint ones) in a graph, and a “cycle remover” algorithm (Supplementary Section S2) to move out of directed cycles such that the proposed graph is free of directed cycles. It is plausible that when proposing a new graph, our MCMC algorithm may propose a graph with one or more directed cycles, try to move out of these directed cycles only to generate a graph with different directed cycles. Therefore, our algorithm may need to repeatedly identify and remove directed cycles in one MCMC iteration. However, since we

focus on relatively small graphs in this paper, this scenario is rather unlikely.

Recall that our algorithm next calculates the acceptance probability for the proposed graph relative to the current one. Although the (repeated) removal of directed cycles enters the calculation of the transition probability between the current and proposed graph, the probabilities involving the cycles are in the end canceled in the calculation of the acceptance ratio. Let \mathbf{D} be a vector of indices of the edges that *differ* between the current graph \mathbf{S} and proposed graph \mathbf{S}' and \mathbf{C} be an integer vector where the element c_j represents the number of edges that *can* change state for the edge represented by d_j (see examples in Supplementary Section S3). These two vectors have the same length, denoted by h . The probability of moving from \mathbf{S} to \mathbf{S}' , i.e., $\Pr(\mathbf{S} \rightarrow \mathbf{S}')$, is the product of the probabilities of changes at individual edges in \mathbf{D} , and each of these probabilities further consists of two probabilities: the probability that an edge in the graph is chosen to change states, which is $1/c_j$, and the probability of edge d_j changing from its current state S_{d_j} to the state S'_{d_j} , denoted by $\Pr(S_{d_j} \rightarrow S'_{d_j})$. Therefore,

$$\Pr(\mathbf{S} \rightarrow \mathbf{S}') = \prod_{j=1}^h \frac{1}{c_j} \Pr(S_{d_j} \rightarrow S'_{d_j}) = \prod_{j=1}^h \frac{1}{c_j} \prod_{j=1}^h \Pr(S_{d_j} \rightarrow S'_{d_j}). \quad (8)$$

We prove that the transition probabilities do not depend on the path taken from the current graph to the proposed graph (the process of introducing and removing directed cycles) but only on the edges that have different states between the two graphs.

Theorem 1 *When calculating the acceptance probability, α , the transition probability between the current and proposed graph, $\Pr(\mathbf{S} \rightarrow \mathbf{S}')$ and $\Pr(\mathbf{S}' \rightarrow \mathbf{S})$, depends only on the edges whose states are different between the two graphs.*

PROOF See Supplementary Section S4 for the proof and S3 for examples. ■

3 Relationships to existing MCMC methods

We compare baycn to four existing Bayesian MCMC methods for inferring DAGs: two structure-based methods and two order-based methods (Table 1). The structure-based methods, which include a Gibbs sampler (Goudie and Mukherjee, 2016) and MC³ (Madigan et al., 1995; Goudie and Mukherjee, 2016), are similar to baycn and sample the graph space based on edges. The Gibbs sampler considers a DAG as a set of parent nodes and moves through the graph space by proposing new parents for a subset of nodes. At each iteration of the MC³ algorithm a proposal graph is selected from all neighbor graphs, each of which has one edge more or less than the current graph. The order-based methods include order MCMC a method based on node orderings (Friedman and Koller, 2003; Kuipers et al., 2018) and partition MCMC which is based on node partitions (Kuipers and Moffa, 2017). A DAG leads to one distinct node partition, but one node partition may correspond to multiple DAGs. On the other hand, a node partition may imply multiple node orderings and is a more succinct representation of a DAG than a node ordering. These methods propose a new order or partition by moving one node in the current order or by splitting or joining the current partition.

Our method differs from these existing methods in two ways. First, although all the Bayesian methods directly or indirectly estimate the posterior probabilities of the adjacency matrix, our method requires that the prior probabilities of the edge states are specified (for example, $p_0 = 0.05$, $p_1 = 0.05$, and $p_2 = 0.9$). With this specification, we can assess if the data support an edge state

by examining how much the posterior has changed from the prior. The other methods do not specify such a prior, thus making it difficult to interpret the posterior probabilities. Second, baycn, Gibbs and MC³ explore only among the edges in the candidate graph, whereas the two order-based methods allow for inclusion of other edges.

Table 1: Summary of our method and four other Bayesian methods for inference of DAGs

	bayen	Gibbs (Goudie and Mukherjee, 2016)	MC ³ (Madigan et al., 1995)	order MCMC (Friedman and Koller, 2003; Kuipers et al., 2018)	partition MCMC(Kuipers and Moffa, 2017)
Input	Data matrix, adjacency matrix, prior on edge states	Data matrix, a list of edges to always/never consider can be specified, prior on graph space	Data matrix, a list of edges to always/never consider can be specified, prior on graph space	Data matrix, edges to be considered, the parameters to calculate the graph score	Data matrix, edges to be considered, the parameters to calculate the graph score
Output	Posterior probabilities of three edge states	Posterior probabilistic adjacency matrix	Posterior probabilistic adjacency matrix	Posterior probabilistic adjacency matrix	Posterior probabilistic adjacency matrix
Type of Sampling	Edges and edge directions	Edges and edge directions	Edges and edge directions	Node orderings	Node partitions
MCMC Move	Select a subset of edges and change their states	Select a subset of nodes and change their parent nodes	Add or remove an edge	Move a node to a new position	Split an existing partition or merge two partitions

4 Simulation Study

4.1 Data Simulation

We simulated data under seven different topologies with different numbers of nodes, edges and v structures (Figures 1 and 2). Graphs M1 (not a v structure and having two other Markov equivalent graphs; Figure 1a) and M2 (a v structure; Figure 1b) are among the building blocks of more complex DAGs. Both GN4 and GN5 (Figure 2a) contain M1 and M2 as subgraphs, and their skeletons allow for directed cycles. The Supplementary Figures S3 and S5 show examples of the Markov equivalence classes for topologies GN4 and GN5. These graphs test the ability of baycn to find and remove directed cycles from the inferred graph. The multi-parent graph (Figure 2c) contains three v structures. Graph GN11 (Figure 2d) contains one v structure but more edges with Markov equivalent edges. Graph GN8 (Figure 2e) is more complex than previous graphs, containing two v structures and allowing for three overlapping directed cycles.

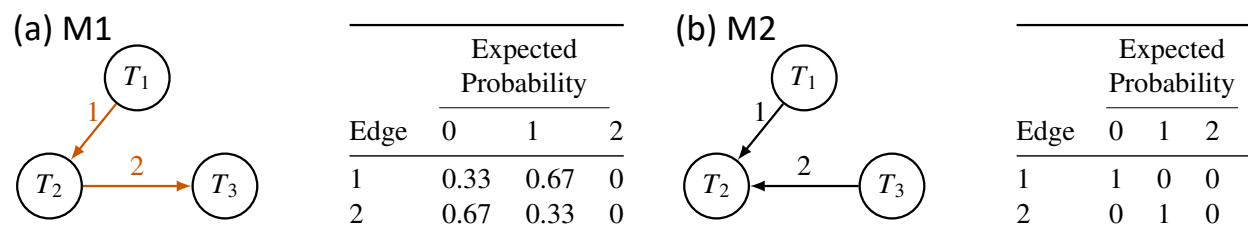


Figure 1: Two graphs used in simulation studies and expected probabilities for each accounting for Markov equivalence. (a) M1 has two other Markov equivalent graphs. The orange edges indicate edges whose direction cannot be uniquely determined. (b) M2 is a v structure and can be uniquely determined.

For all of our simulations we generated data for each node under a normal distribution with the mean following a linear model (Equation 6). For simplicity, we set all the variance to one, all the intercept β_0 to zero and all other β s to take the same value. The signal in the data is primarily reflected in the latter, which we refer to as the signal strength. The signal strength has three values 0.2 (weak signal), 0.5 (moderate signal), and 1 (strong signal). We also consider three sample sizes: 100, 200 and 600. For each topology we simulated 25 data sets under each of the nine different combinations of signal strength and sample size.

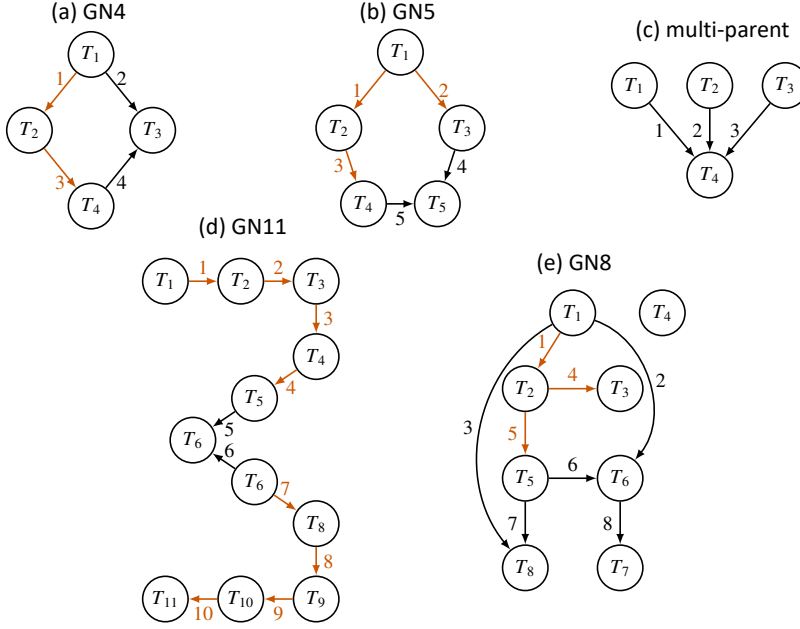


Figure 2: Five additional graphs used in simulation studies. The subgraphs consisting of orange edges have Markov equivalent graphs and cannot be uniquely determined.

4.2 Performance assessment of methods

We assess the performance and compare methods using the following metrics:

1. The edge-wise Mean Squared Error (eMSE): for an edge j , we calculate the MSE between the expected and posterior probabilities of the three states:

$$\text{eMSE}_j = \frac{1}{3} \sum_{k=0}^2 [\Pr(S_j = k) - \Pr(S_j = k | \mathbf{T})]^2, \quad (9)$$

where $\Pr(S_j = k)$ is the expected probability under Markov equivalence. This metric informs us which edges are more accurately inferred and which ones are not.

2. The MSE for the whole graph based on three possible edge states: this is the eMSE averaged over all m edges in the graph:

$$\text{MSE}_1 = \frac{1}{m} \sum_{j=1}^m \text{eMSE}_j = \frac{1}{3m} \sum_{j=1}^m \sum_{k=0}^2 [\Pr(S_j = k) - \Pr(S_j = k | \mathbf{T})]^2. \quad (10)$$

3. The MSE between the expected and posterior probabilistic adjacency matrix on all m edges. This metric is essentially the same as MSE_1 , but makes it easy to compare with other Bayesian methods.

$$\text{MSE}_2 = \frac{1}{2m} \sum_{\substack{(j,k) \text{ or} \\ (k,j) \in \mathbf{E}}} \left\{ [\Pr(A_{jk} = 1) - \Pr(A_{jk} = 1 | \mathbf{T})]^2 + [\Pr(A_{kj} = 1) - \Pr(A_{kj} = 1 | \mathbf{T})]^2 \right\}. \quad (11)$$

For baycn, we use the posterior probability for state 0 and state 1 in place of $\Pr(A_{jk} = 1 | \mathbf{T})$

and $\Pr(A_{kj} = 1 \mid \mathbf{T})$ respectively.

4. The MSE between the expected and posterior probabilistic adjacency matrix on all $(b^2 - b)/2$ possible edges among the b nodes in the graph.

$$\text{MSE}_3 = \frac{1}{b^2 - b} \sum_{j=1}^b \sum_{k=1}^b [\Pr(A_{jk} = 1) - \Pr(A_{jk} = 1 \mid \mathbf{T})]^2. \quad (12)$$

This metric is helpful to assess how likely a method is to infer edges outside the candidate graph. If the candidate graph is the skeleton of the true graph, then this metric quantifies the extent to which false positive edges are inferred.

5. Precision and power for the whole graph. Precision measures how many of the inferred edges are in the true graph and power measures how many of the inferred edges are true edges.

$$\text{Precision} = 1 - \text{FDR} = \frac{\# \text{ of true edges inferred}}{\# \text{ of inferred edges}}, \quad (13)$$

$$\text{Power} = \frac{\# \text{ of true edges inferred}}{\# \text{ of edges in true graph}}. \quad (14)$$

To calculate these metrics, we will apply a cutoff of 0.5 to the posterior probability of an edge being present, which is the sum of the probability of both directions. These metrics ignore the nuances in the probabilities, but as percentages, they are easy to interpret and provide a quick indication of the inference accuracy.

4.3 Results from using the true graph skeleton as the candidate graph

For all the topologies we ran baycn once per simulated data set and used a burn-in of 20%. For topologies M1, M2, GN4, GN5, and multi-parent we ran baycn for 3×10^4 iterations with a step size of 120 and for topologies GN8 and GN11 we ran baycn for 5×10^4 iterations with a step size of 200. We used the probability $(p_0, p_1, p_2) = (0.05, 0.05, 0.9)$ as the prior for edge states. We assess the performance with MSE_1 (Equation 10).

In general, the performance of baycn depends on the signal strength β , the sample size N , and the complexity of the graph. As expected, for each topology MSE_1 decreases as both N and β increase (Table 2). Between the signal strength and sample size, the former has a larger effect on MSE_1 , because for all seven topologies the MSE is much lower for a strong signal and small sample size than for a weak signal and large sample size. A close examination of the graphs inferred for different values of MSE_1 shows that an MSE_1 of below 0.1 typically corresponds to accurate inference: the direction of all the edges is correctly inferred, and the relative magnitude of the posterior probabilities of the three states for any edge is similar to that of the expected probabilities. Using this guideline, we observe that baycn performs well on GN4 and GN5 even with a weak signal, as long as the sample size is large, indicating that baycn can find and remove directed cycles from the graph. In GN11 baycn can also correctly identify the edge directions in smaller subgraphs separated by a v structure. For both M2 and multi-parent topologies that contain one or more v structures, MSE_1 is nearly perfect at moderate to strong levels of β but is larger at a weak signal than that for any other topology with the same sample size. This is consistent with our observation that it is generally difficult for existing graph inference algorithms to correctly

identify v structures with a weak signal (Badsha and Fu, 2019; Badsha et al., 2018). Additionally, for all combinations of N and β , except for topologies M2 and multi-parent with a weak signal, baycn performs the worst on GN8, the most complex topology in our simulation, suggesting that the complexity of the graph strongly influences the performance of baycn.

Table 2: Performance of baycn on all the graphs in simulation. Features of the graphs, such as the number of edges and v structures, are listed. The mean and standard deviation of MSE_1 (Equation 10), sample size N , and signal strength β are also listed, For each simulation scenario we generated 25 independent data sets and ran baycn once on each data set.

Topology	#edges	#v structures	N	MSE					
				$\beta = 0.2$		$\beta = 0.5$		$\beta = 1$	
				mean	sd	mean	sd	mean	sd
M1	2	0	100	0.1796	0.0949	0.0127	0.0353	0.0011	0.0016
			200	0.0734	0.074	0.0014	0.0015	0.0012	0.0013
			600	0.0237	0.0326	0.001	0.0009	0.0008	0.0007
M2	2	1	100	0.3384	0.1081	0.0909	0.0919	0	0
			200	0.2688	0.0881	0.0597	0.082	0	0
			600	0.1323	0.0735	0	0	0	0
GN4	4	1	100	0.2731	0.0711	0.0674	0.0417	0.01	0.0276
			200	0.167	0.0554	0.0755	0.0639	0.0046	0.0142
			600	0.0839	0.0259	0.0503	0.0602	0.0069	0.0182
GN5	5	1	100	0.2687	0.0785	0.0396	0.0465	0.0022	0.0023
			200	0.1562	0.049	0.0171	0.0235	0.002	0.0031
			600	0.0684	0.0338	0.0114	0.0483	0.002	0.0024
Mult-parent	3	3	100	0.3361	0.0961	0.0486	0.0698	0	0
			200	0.237	0.0812	0.0032	0.0135	0	0
			600	0.1418	0.0625	0	0.0002	0	0
GN11	10	1	100	0.2266	0.0513	0.0353	0.0225	0.0042	0.0031
			200	0.139	0.0431	0.0121	0.0162	0.0066	0.0041
			600	0.0613	0.0197	0.0047	0.0043	0.0046	0.0039
GN8	8	2	100	0.2932	0.0437	0.0656	0.028	0.0191	0.0366
			200	0.1945	0.0449	0.0868	0.0528	0.0432	0.0694
			600	0.1155	0.0541	0.067	0.0661	0.0201	0.0457

4.4 Results on the identification of false positive edges

For this assessment we include a false edge in M1, M2 and GN4, and two false edges in the larger GN11 (Supplementary Figure S9). These false edges lead to the possibility of generating one or more directed cycles in the graph during MCMC, making the identification of false edges more challenging. We used the same data generated in the previous section for these topologies (without false edges) and ran baycn with the candidate graph being the true graph skeleton plus the false edges. We calculated eMSE (Equation 9) to assess the edge-wise performance. We explored the

impact of three edge-state priors on the inference, with an increasing probability of the edge being absent: prior 1: $(p_0, p_1, p_2) = (1/3, 1/3, 1/3)$; prior 2 $(p_0, p_1, p_2) = (0.25, 0.25, 0.5)$, and prior 3: $(p_0, p_1, p_2) = (0.05, 0.05, 0.9)$ (previously used in Section 4.3).

Once again using $\text{MSE} < 0.1$ as the criterion for correct inference, we observed that baycn can identify false positive edges under prior 3, which assigns a large prior probability to absence (Supplementary Tables S1 - S4). In all four graphs the eMSE for the false edges decreases as p_2 increases. On the other hand, the edge probabilities of the true edges are generally estimated correctly under all three priors and for different signal strengths or sample sizes, even when the false edges are not properly identified and have a large eMSE (Supplementary Tables S1 - S4). The impact of the prior on the true edges is more complex: in M1 and M2 the eMSE for true edges decreases as p_2 increases, whereas in GN4 and GN11 the eMSE for the true edges follows an opposite trend in some cases. This may be due to the amount of information in the data and the expected edge state probabilities. With sufficient information in the data, it does not matter much which prior is used, the posterior probabilities for the true edges are close to the expected ones. However, if the information in the data is insufficient but the prior happens to be close to the expectation, then the posterior probabilities will be close to the prior and result in a small eMSE. In summary, this investigation confirms that prior 3 is the prior of choice, as it balances the need to detect false positive edges and to correctly infer the true edges. We have primarily used prior 3 in other simulations.

4.5 Comparison with existing Bayesian MCMC methods

We compare baycn with other Bayesian methods using the true graph skeleton as the input. We focus on GN4, GN8 and GN11, which have different levels of complexity (Figure 2; Supplementary Tables S6 and S7). We ran all the methods for 3×10^4 iterations on GN4 and for 5×10^4 iterations on GN8 and GN11. We used a burn-in of 20% for all the methods. We set the step size in baycn to be 120 for GN4 and 200 for GN8 and GN11. We used the default step size for order and partition MCMC which is calculated by # of iterations/1000. This results in the step size being 30 for GN4 and 50 for GN8 and GN11. Gibbs and MC^3 use all of the iterations after the burn-in.

Using MSE_2 (Equation 11) as the metric, which evaluates the deviation from the expected probabilistic adjacency matrix on true edges, we observed that all five methods have similar MSE_2 , with MC^3 having larger mean MSE_2 and larger variation (Figure 3a). Since the signal strength is crucial to the performance (Section 4.3), we grouped the results by signal strength, and observed that as expected, MSE_2 decreases as the signal strength increases for each method in general (Figure 3b). However, MC^3 produced higher MSE_2 for two of the three topologies (GN4 and GN8) at $\beta = 1$ than at $\beta = 0.5$, which leads to the large variation for MC^3 at $\beta = 1$. Additionally, order and partition MCMC performed worse than others at weak signal. The complexity of the graph also strongly influences the inference accuracy (Section 4.3). Grouping the results by topologies, we observed that MSE_2 is generally small for GN11, which contains only one v structure despite having the largest number of nodes. MC^3 performs worse than others on GN4 and GN8, both of which can easily generate directed cycles during MCMC. baycn and other methods perform similarly on the three topologies, with partition MCMC being slightly worse for GN11. In summary, across different simulation scenarios, baycn and Gibbs show similar and better performance than other methods. Partition and order MCMC are slightly worse in some cases, whereas MC^3 is the least accurate and least stable among the five methods.

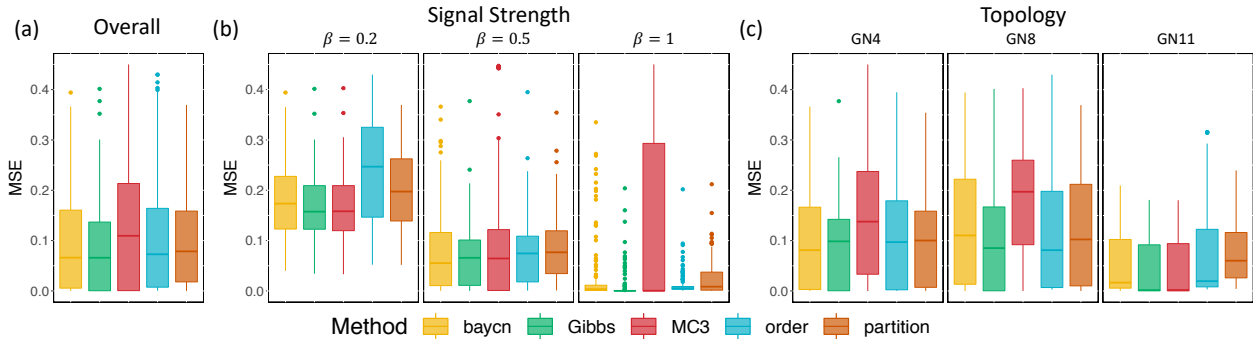


Figure 3: Boxplots of MSE_2 (Equation 11) for baycn and other Bayesian methods for topologies GN4, GN8, and GN11 with varying signal strengths and sample sizes. The true graph skeleton was used as the input. (a) The overall MSE_2 grouped by method. (b) MSE_2 grouped by method and signal strength β . (c) MSE_2 grouped by method and topology. Also see Supplementary Table S6.

Whereas baycn considers only edges in the candidate graph, both order and partition MCMC allow for inclusion of additional edges and can estimate substantial posterior probability for those edges. To assess the overall inclusion of false edges, we also calculated MSE_3 on all possible edges in each graph for each method from the simulations above. Results from this evaluation (Supplementary Figure S10 and Table S7) lead to observations similar to those under MSE_2 , indicating that although these methods may include false edges, posterior probabilities for these edges are small overall.

Although it is more efficient to use baycn with a sparse candidate graph as input, we are interested in whether baycn can run on a fully connected graph and how its performance compares with other methods. We calculated precision, power and MSE_2 for this evaluation. Precision is nearly perfect for all the methods in most of the simulation scenarios (Figure 4). Power is also nearly 100% for both moderate and strong signals (Figure 4). However, for data sets with a weak signal ($\beta = 0.2$), the power is low especially at a lower sample size (Supplementary Table S5), resulting in a large variation in power with this signal strength for all the methods (Figure 4). However, order MCMC has even lower power on average and partition MCMC has larger variation than other methods at $\beta = 0.2$, as they tend to infer a higher posterior probability for edge absence and therefore infer fewer true edges as present (see examples in Supplementary Tables S9-S11). In terms of the MSE, similar to our observation in Section 4.3, MSE_2 for each method decreases as the signal strength or sample size increases (Supplementary Table S5) and is influenced more by the signal strength than by the sample size. Also similar to the results on power, we observe that order and partition MCMC have higher mean or larger variation than other methods at low signal strength. We also note that Gibbs and MC³ have slightly higher mean MSE_2 with a strong signal ($\beta = 1$).

Our MCMC algorithm is also fast. To compare the runtime of the five algorithms we used the data simulated for GN4, GN8, and GN11 with $\beta = 1$ and $N = 600$. We ran each algorithm once per data set on an Intel Xeon D-1540 2.00 GHz processor with 128 GB of memory (see runtime in Supplementary Table S8). On all three topologies, order MCMC is the fastest, followed closely by baycn and partition MCMC. baycn is approximately three times as fast as MC³ and can be 50 times as fast as Gibbs. On the larger topology GN11, baycn is slightly faster than partition MCMC.

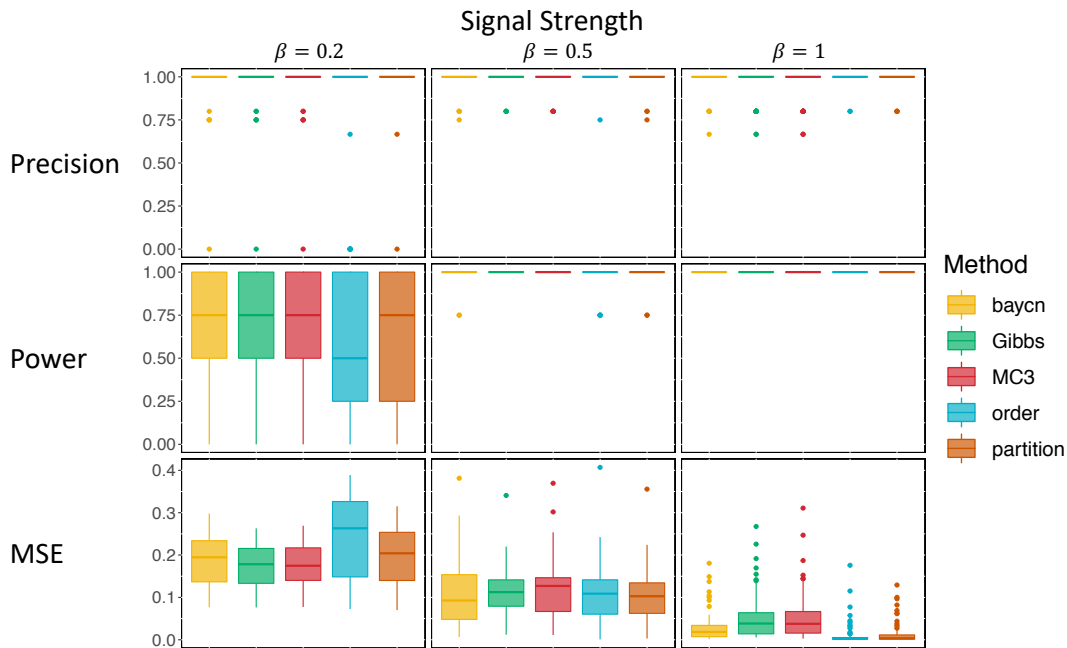


Figure 4: Boxplots of precision, power, and MSE_2 (Equation 11) of baycn and other Bayesian methods for GN4 when a fully connected graph was used as the input. Precision, power, and MSE_2 are grouped by method and signal strength β . Also see Supplementary Table S5.

5 Discussion

Here we present our Bayesian approach to DAG inference. We have developed a novel and coherent definition of the edge state and used this definition to represent a DAG. The posterior probabilities of edge states are therefore much easier to interpret than those of existing methods. We have developed an MCMC algorithm for sampling under this representation. Our algorithm deals with directed cycles and accounts for Markov equivalence. We have demonstrated through simulation studies that baycn is fast and can accurately estimate the edge probabilities in general, and that it performs as well as or better than current MCMC methods. With a suitable prior of edge states, baycn can correctly estimate edge probabilities both when the true graph skeleton is the input and when false edges are included in the input.

In the method comparison we used two types of MSE to assess the deviation from the expected probabilistic adjacency matrix (MSE_2 on only the true edges and MSE_3 on all possible edges). MSE_2 favors the two order-based methods, as these methods allow for additional edges outside the true skeleton and MSE_2 ignores these false positive edges. In comparison, MSE_3 favors the structure-based methods, since only the true edges enter the calculation when the true graph skeleton is used as input. Despite this difference, the two MSEs show similar patterns in our simulation studies.

We also used 0.5 as the cutoff value for the posterior probability of edge presence when calculating precision and power. This value is a natural choice for other Bayesian methods under comparison, since the prior probabilities are generally unspecified. With baycn, 0.5 can be over conservative, especially when prior 3 of $(p_0, p_1, p_2) = (0.05, 0.05, 0.9)$ is used. Under this prior, a posterior probability of say, 0.2, for each of the two directions can already indicate strong evidence for edge presence, even though the edge presence probability is 0.4 in this case. However, precision and power for baycn with such a conservative cutoff are still nearly perfect in most cases and

comparable to or better than other methods in other cases. This again confirms that baycn performs satisfactorily in our simulation.

6 Supplementary Materials

Supplementary file: Additional tables, figures, algorithms, and proofs that supplement the main article (supplementaryMaterial.pdf).

R code: The method developed here is implemented in our R package baycn – <https://github.com/evanamartin/baycn>.

Other Bayesian methods we compared with are available in the following R packages: order and partition MCMC (the BiDAG package) – <https://CRAN.R-project.org/package=BiDAG>.

MC³ and Gibbs (the structmcmc package) – <https://github.com/rjbgoudie/structmcmc>.

Simulated data: Simulated data sets for this paper are available also on GitHub – https://github.com/evanamartin/baycn_simulations.

7 Acknowledgements

The authors thank Robert J. B. Goudie for helping with the Gibbs sampler implemented in his structmcmc R package.

Supplementary Materials

Note: All of the references to equations and figures in Sections S1 - S4 refer to equations and figures in the Supplementary Materials file and not in the main text.

S1 Identifying directed cycles

1. Find the nodes that are connected to two or more nodes as a cycle contains at least three nodes and each node in a cycle has at least one incoming edge and one outgoing edge. To do so, we use the following steps:
 - i. Add the adjacency matrix to its transpose.
 - ii. Sum each row and delete rows (the row indices are preserved) with a sum less than 2.
 - iii. Apply the following rule to the adjacency matrix

$$\forall A_{j,k} = 1, \begin{cases} A_{j,k} = 0 & \text{if } k \notin J \\ A_{j,k} = 1 & \text{if } k \in J, \end{cases}$$

where J is the set of remaining row indices in the adjacency matrix.

- iv. Repeat steps ii and iii until $\forall A_{j,k} = 1, k \in J$ or the reduced adjacency matrix has two or fewer rows.
2. Create a tree as deep as possible starting with the node (i.e., root node) whose index is in the first row of the reduced adjacency matrix. To do this we create a branch, which is a vector of node indices, for each of the nodes (i.e., child nodes) connected to the root. For each branch

we add the index of the child node to the end of the vector, repeating the process of a child node becoming the parent node, until we add an index that has been added to the branch previously. If a parent node has two or more children a new branch is created for each child node.

3. Remove the nodes from the branches that do not belong to the cycle. In addition to the nodes that create a cycle a branch may also contain nodes outside the cycle. To remove these nodes, we start at the last node (i.e., the leaf) of the branches created in the previous step and work up the branch until we come to a node index that matches the leaf. Nodes above this node are then removed. For example, a branch may be (3, 4, 1, 6, 5, 2, 1) and the trimmed branch would be (1, 6, 5, 2, 1).
4. Convert the trimmed branches of a cycle into a vector of adjacency matrix coordinates by pairing up the adjacent nodes in each trimmed branch to produce a vector of edge coordinates. For example, if a trimmed branch is (1, 6, 5, 2, 1) then the adjacency matrix coordinates for the edges between the nodes in the cycle are ((1, 6), (6, 5), (5, 2), (2, 1)).
5. Generate a vector of edge states from the vector of edge coordinates by considering each pair of coordinates and comparing the first number to the second number. If the first number is smaller than the second number the edge state is 0, indicating that the edge points from the node with a smaller index to the node with the larger index. If the first number is larger than the second number the edge state is 1, indicating that the edge points from the node with a larger index to the node with a smaller index. The coordinates vector from the example in Step 4 is ((1, 6), (6, 5), (5, 2), (2, 1)) and the edge states that form a directed cycle are (0, 1, 1, 1).
6. Use the vector of edge coordinates from step 4 to create a vector of edge indices. For example, the edge indices for the coordinates ((1, 6), (6, 5), (5, 2), (2, 1)) are (2, 6, 5, 1).
7. Define each cycle by the number of edges in the cycle and a decimal number calculated using the vector of edge states (step 5) and the vector of edge indices (step 6). The decimal number for the j th cycle is calculated by

$$\sum_{k=1}^m \mathbf{1}_{Q_j}(S_k) S_k 3^k, \quad (1)$$

where

$$\mathbf{1}_{Q_j}(S_k) = \begin{cases} 1 & \text{if } S_k \in Q_j \\ 0 & \text{if } S_k \notin Q_j. \end{cases} \quad (2)$$

The vector, Q_j , is the set of edges that make up cycle j , S_k is the state of edge k , and m is the number of edges in the network.

For example, Figure 1 shows a graph with two cycles nested within a larger cycle. If the edges are oriented as shown in the figure the decimal number for the cycle involving edges (2, 3, 5, 6, 7) with states $\mathbf{S} = (0, 1, 0, 0, 0)$ is

$$0(0 \times 3^1) + 1(0 \times 3^2) + 1(1 \times 3^3) + 0(0 \times 3^4) + 1(0 \times 3^5) + 1(0 \times 3^6) + 1(0 \times 3^7) = 9,$$

and the decimal number for the cycle involving edges (1, 3, 4, 5, 6, 7) with states $\mathbf{S} = (0, 1, 0, 0, 0, 0)$ is

$$1(0 \times 3^1) + 0(0 \times 3^2) + 1(1 \times 3^3) + 1(0 \times 3^4) + 1(0 \times 3^5) + 1(0 \times 3^6) + 1(0 \times 3^7) = 9.$$

Because two different cycles can have the same decimal number we also group the cycles by the number of edges in the cycle. By grouping cycles this way we are able to distinguish between the two cycles in the example above because the first cycle has 5 edges and the second cycle has 6 edges.

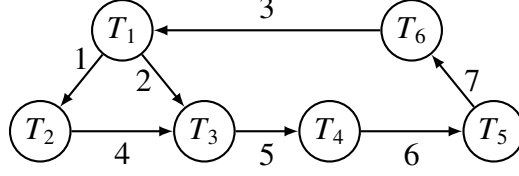


Figure 1: A graph with two directed cycles one cycle is made up of edges {2, 5, 6, 7, 3} and the other with edges {1, 4, 5, 6, 7, 3}. The two cycles have four edges in common.

S2 Removing Directed Cycles

1. For the current graph calculate the decimal for each set of edges that could form a directed cycle following Equation (1).
2. Compare the number of edges and the decimal, for each set of edges that could form a directed cycle, to the list of decimals and number of edges for the directed cycles.
3. For each directed cycle, randomly select an edge and change it from its current state to a different state according to the prior probability of edge states.
4. Repeat steps 1 - 3 until there are no directed cycles in the graph.

S3 Examples of Theorem 1

Example 1 – One directed cycle

Consider the current graph in Figure 2a with states $\mathbf{S} = (0, 0, 0, 1, 1)$ and the proposed graph in Figure 2c with states $\mathbf{S}' = (0, 1, 2, 1, 1)$. Edges #2 and #3 have different states between \mathbf{S} and \mathbf{S}' therefore $\mathbf{D} = 2, 3$. There are two different paths to move from \mathbf{S} to \mathbf{S}' . In path 1 there are two steps: i) edge #2 changes direction which creates a directed cycle between nodes T_1 , T_2 , and T_3 (Figure 2b) and ii) the directed cycle is removed by edge #3 changing from state 0 to 2. In path 2 edges #2 and #3 change states in one step. If the prior on edge states is $p_0 = 0.05$, $p_1 = 0.05$ and $p_2 = 0.9$ then the probabilities for the two paths are

$$\text{path 1: } \Pr(S_{d_2} \rightarrow S'_{d_2}) = \frac{0.05}{0.95}, \Pr(S_{d_3} \rightarrow S'_{d_3}) = \frac{0.9}{0.95}, \mathbf{C}^1 = 5, 3$$

and

$$\text{path 2: } \Pr(S_{d_2} \rightarrow S'_{d_2}) = \frac{0.05}{0.95}, \Pr(S_{d_3} \rightarrow S'_{d_3}) = \frac{0.9}{0.95}, \mathbf{C}^2 = 5, 5.$$

Combining the probabilities from each path we obtain the transition probability of moving to the proposed graph:

$$\Pr(\mathbf{S} \rightarrow \mathbf{S}') = \frac{1}{5} \frac{1}{3} \frac{0.05}{0.95} \frac{0.9}{0.95} + \frac{1}{5} \frac{1}{5} \frac{0.05}{0.95} \frac{0.9}{0.95} = \left(\frac{1}{5} \frac{1}{3} + \left(\frac{1}{5} \right)^2 \right) \frac{0.05}{0.95} \frac{0.9}{0.95}. \quad (3)$$

Any directed cycle created when moving from \mathbf{S} to \mathbf{S}' needs to be created when moving from \mathbf{S}' to \mathbf{S} . Therefore, when moving from \mathbf{S}' to \mathbf{S} there are also two paths. Path 1 is made up of two steps: i) edge #3 changes from state 2 to 0 creating a cycle between nodes T_1 , T_2 , and T_3 and ii) the cycle is removed by changing edge #2 from state 1 to 0. For path 2 edges #2 and #3 both change states in one step. The probabilities for the paths are

$$\text{path 1: } \Pr(S'_{d_2} \rightarrow S_{d_2}) = \frac{0.05}{0.95}, \Pr(S'_{d_3} \rightarrow S_{d_3}) = \frac{0.05}{0.1}, \mathbf{C}^{1'} = 5, 3$$

and

$$\text{path 2: } \Pr(S'_{d_2} \rightarrow S_{d_2}) = \frac{0.05}{0.95}, \Pr(S'_{d_3} \rightarrow S_{d_3}) = \frac{0.05}{0.1}, \mathbf{C}^{2'} = 5, 5.$$

The transition probability of moving back to the current graph is

$$\Pr(\mathbf{S}' \rightarrow \mathbf{S}) = \frac{1}{5} \frac{1}{3} \frac{0.05}{0.95} \frac{0.05}{0.1} + \frac{1}{5} \frac{1}{5} \frac{0.05}{0.95} \frac{0.05}{0.1} = \left(\frac{1}{5} \frac{1}{3} + \left(\frac{1}{5} \right)^2 \right) \frac{0.05}{0.95} \frac{0.05}{0.1}. \quad (4)$$

The term $\frac{1}{5} \frac{1}{3} + \left(\frac{1}{5} \right)^2$ in equations 3 and 4 cancels out when calculating the acceptance probability, α , and we are left with the probability of moving between the states that differ between the current graph (Fig 2a) and the proposed graph (Fig 2c). More generally, we can apply the same procedure to traverse the paths between any two graphs.

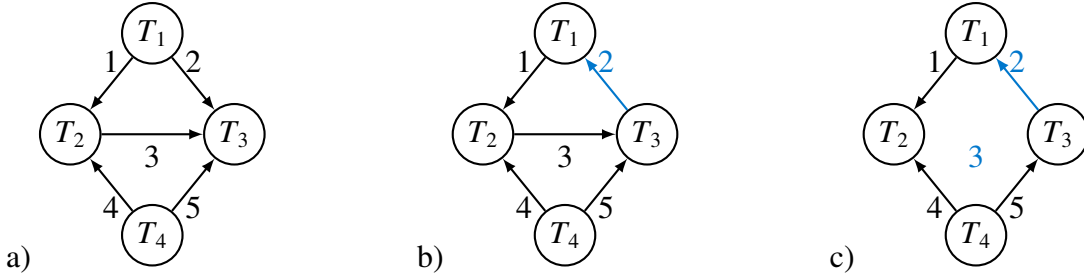


Figure 2: The graphs for example 1. a) The current graph. b) An intermediate graph between the current graph and the proposed graph where a directed cycle has been introduced into the network. c) The proposed graph.

Example 2 – Multiple directed cycles

We show a second more complex example below. If we start with the graph in Figure 3a with states $\mathbf{S} = (0, 0, 0, 1, 1)$ and the proposed graph in Figure 3d with states $\mathbf{S}' = (2, 1, 1, 1, 0)$ there are four edges with different states between the two graphs and $\mathbf{D} = 1, 2, 3, 5$. There are three different paths to move from \mathbf{S} to \mathbf{S}' . The steps in path 1 are: i) edges #2 and #5 change directions creating two directed cycles, the first cycle is between nodes T_1 , T_2 , and T_3 and the second cycle is between nodes T_2 , T_3 , and T_4 (Figure 3b), ii) edge #1 changes from state 0 to 2 removing the first cycle (Figure 3c), and iii) edge #3 changes direction which removes the second cycle (Figure 3d). The steps in path 2 are: i) edges #1, #2, and #5 all change states creating one directed cycle between nodes T_2 , T_3 , and T_4 (Figure 3c) and ii) edge #3 changes direction removing the cycle. In path 3 edges #1, #2, #3, and #5 all change states in one step. If the prior on edge states is $p_0 = 0.05$,

$p_1 = 0.05$, and $p_2 = 0.9$ then the probabilities for the three paths are:

$$\begin{aligned} \text{path 1: } \Pr(S_{d_1} \rightarrow S'_{d_1}) &= \frac{0.9}{0.95}, \Pr(S_{d_2} \rightarrow S'_{d_2}) = \frac{0.05}{0.95}, \Pr(S_{d_3} \rightarrow S'_{d_3}) = \frac{0.05}{0.95}, \\ &\Pr(S_{d_5} \rightarrow S'_{d_5}) = \frac{0.05}{0.95}, \mathbf{C}^1 = 5, 5, 3, 3, \end{aligned}$$

$$\begin{aligned} \text{path 2: } \Pr(S_{d_1} \rightarrow S'_{d_1}) &= \frac{0.9}{0.95}, \Pr(S_{d_2} \rightarrow S'_{d_2}) = \frac{0.05}{0.95}, \Pr(S_{d_3} \rightarrow S'_{d_3}) = \frac{0.05}{0.95}, \\ &\Pr(S_{d_5} \rightarrow S'_{d_5}) = \frac{0.05}{0.95}, \mathbf{C}^2 = 5, 5, 5, 3, \end{aligned}$$

and

$$\begin{aligned} \text{path 3: } \Pr(S_{d_1} \rightarrow S'_{d_1}) &= \frac{0.9}{0.95}, \Pr(S_{d_2} \rightarrow S'_{d_2}) = \frac{0.05}{0.95}, \Pr(S_{d_3} \rightarrow S'_{d_3}) = \frac{0.05}{0.95}, \\ &\Pr(S_{d_5} \rightarrow S'_{d_5}) = \frac{0.05}{0.95}, \mathbf{C}^3 = 5, 5, 5, 5. \end{aligned}$$

Therefore, the transition probability of moving to the proposed graph is

$$\begin{aligned} \Pr(\mathbf{S} \rightarrow \mathbf{S}') &= \frac{1}{5} \frac{1}{5} \frac{1}{3} \frac{1}{3} \frac{0.9}{0.95} \frac{0.05}{0.95} \frac{0.05}{0.95} \frac{0.05}{0.95} + \frac{1}{5} \frac{1}{5} \frac{1}{5} \frac{1}{3} \frac{0.9}{0.95} \frac{0.05}{0.95} \frac{0.05}{0.95} \frac{0.05}{0.95} + \frac{1}{5} \frac{1}{5} \frac{1}{5} \frac{1}{5} \frac{0.9}{0.95} \frac{0.05}{0.95} \frac{0.05}{0.95} \frac{0.05}{0.95} \\ &= \left(\left(\frac{1}{5} \right)^2 \left(\frac{1}{3} \right)^2 + \left(\frac{1}{5} \right)^3 \frac{1}{3} + \left(\frac{1}{5} \right)^4 \right) \frac{0.9}{0.95} \frac{0.05}{0.95} \frac{0.05}{0.95} \frac{0.05}{0.95}. \end{aligned} \quad (5)$$

As in example 1 any directed cycle that is created when moving from \mathbf{S} to \mathbf{S}' needs to also be created when moving from \mathbf{S}' to \mathbf{S} . There are also three different paths to move back to \mathbf{S} from \mathbf{S}' . In path 1 the steps are: i) edges #1 and #3 change states creating two directed cycles the first cycle is between nodes T_1 , T_2 , and T_3 and the second cycle is between nodes T_2 , T_3 , and T_4 , ii) edge #2 changes direction removing the first cycle, and iii) edge #5 changes direction removing the second directed cycle. Path 2 has two steps i) edges #1, #2 and #3 all change state creating a directed cycle between nodes T_2 , T_3 , and T_4 and ii) edge #5 changes direction removing the cycle. In path 3 there is only one step where edges #1, #2, #3, and #5 all change states. The probabilities for these paths are

$$\begin{aligned} \text{path 1: } \Pr(S'_{d_1} \rightarrow S_{d_1}) &= \frac{0.05}{0.1}, \Pr(S'_{d_2} \rightarrow S_{d_2}) = \frac{0.05}{0.95}, \Pr(S'_{d_3} \rightarrow S_{d_3}) = \frac{0.05}{0.95}, \\ &\Pr(S'_{d_5} \rightarrow S_{d_5}) = \frac{0.05}{0.95}, \mathbf{C}^{1'} = 5, 5, 3, 3, \end{aligned}$$

$$\begin{aligned} \text{path 2: } \Pr(S'_{d_1} \rightarrow S_{d_1}) &= \frac{0.05}{0.1}, \Pr(S'_{d_2} \rightarrow S_{d_2}) = \frac{0.05}{0.95}, \Pr(S'_{d_3} \rightarrow S_{d_3}) = \frac{0.05}{0.95}, \\ &\Pr(S'_{d_5} \rightarrow S_{d_5}) = \frac{0.05}{0.95}, \mathbf{C}^{2'} = 5, 5, 5, 3, \end{aligned}$$

and

$$\begin{aligned} \text{path 3: } \Pr(S'_{d_1} \rightarrow S_{d_1}) &= \frac{0.05}{0.1}, \Pr(S'_{d_2} \rightarrow S_{d_2}) = \frac{0.05}{0.95}, \Pr(S'_{d_3} \rightarrow S_{d_3}) = \frac{0.05}{0.95}, \\ \Pr(S'_{d_5} \rightarrow S_{d_5}) &= \frac{0.05}{0.95}, \mathbf{C}^{3'} = 5, 5, 5, 5. \end{aligned}$$

Therefore, the transition probability of moving back to the current graph is

$$\begin{aligned} \Pr(\mathbf{S}' \rightarrow \mathbf{S}) &= \frac{1}{5} \frac{1}{5} \frac{1}{3} \frac{1}{3} \frac{0.05}{0.1} \frac{0.05}{0.95} \frac{0.05}{0.95} \frac{0.05}{0.95} + \frac{1}{5} \frac{1}{5} \frac{1}{3} \frac{0.05}{0.1} \frac{0.05}{0.95} \frac{0.05}{0.95} \frac{0.05}{0.95} + \frac{1}{5} \frac{1}{5} \frac{1}{5} \frac{0.05}{0.1} \frac{0.05}{0.95} \frac{0.05}{0.95} \frac{0.05}{0.95} \\ &= \left(\left(\frac{1}{5}\right)^2 \left(\frac{1}{3}\right)^2 + \left(\frac{1}{5}\right)^3 \frac{1}{3} + \left(\frac{1}{5}\right)^4 \right) \frac{0.05}{0.1} \frac{0.05}{0.95} \frac{0.05}{0.95} \frac{0.05}{0.95}. \end{aligned} \quad (6)$$

The term $\left(\frac{1}{5}\right)^2 \left(\frac{1}{3}\right)^2 + \left(\frac{1}{5}\right)^3 \frac{1}{3} + \left(\frac{1}{5}\right)^4$ in equations 5 and 6 cancels out when calculating the acceptance probability, α , and we are left with the probability of moving between the states that differ between the current graph (Fig 3a) and the proposed graph (Fig 3d). More generally, we can apply the same procedure to traverse the paths between any two graphs.

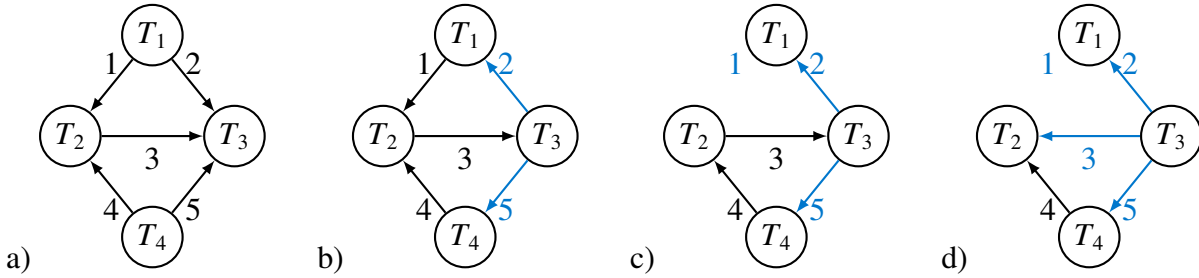


Figure 3: a) The current graph. b) An intermediate graph between the current graph and the proposed graph where two directed cycles have been introduced into the graph. c) An intermediate graph where one of the directed cycles has been removed. d) The proposed graph.

S4 Proof of Theorem 1

Theorem 2 When calculating the acceptance probability, α , the transition probability between the current and proposed graph, $\Pr(\mathbf{S} \rightarrow \mathbf{S}')$ and $\Pr(\mathbf{S}' \rightarrow \mathbf{S})$, depends only on the edges whose states are different between the two graphs.

PROOF Recall that \mathbf{S} is a vector of edge states representing the current graph \mathcal{G} and \mathbf{S}' is a vector of edge states representing the proposal graph \mathcal{G}' . Let \mathbf{D} be a vector of indices of the edges that *differ* between the current graph \mathbf{S} and proposed graph \mathbf{S}' and \mathbf{C} be an integer vector where the element c_j represents the number of edges that *can* change state for the edge represented by d_j . These two vectors have the same length, denoted by h .

We will consider two cases: without and with potential directed cycles in the graph.

Case 1 Without potential directed cycles the probability of moving from the current graph to the

proposed graph is

$$\begin{aligned}\Pr(\mathbf{S} \rightarrow \mathbf{S}') &= \prod_{j=1}^h \frac{1}{c_j} \Pr(S_{d_j} \rightarrow S'_{d_j}) \\ &= \prod_{j=1}^h \frac{1}{c_j} \prod_{j=1}^h \Pr(S_{d_j} \rightarrow S'_{d_j}).\end{aligned}\quad (7)$$

We can use the same procedure of deriving the equation for moving back to the current graph from the proposed graph. Therefore, the probability can be broken down in the same way when moving backwards:

$$\Pr(\mathbf{S}' \rightarrow \mathbf{S}) = \prod_{j=1}^h \frac{1}{c_j} \prod_{j=1}^h \Pr(S'_{d_j} \rightarrow S_{d_j}).\quad (8)$$

Since there are no potential directed cycles in the network the value c_j will always be m which is the number of edges in the network. Therefore, $\prod_{j=1}^h \frac{1}{c_j} = \prod_{j=1}^h \frac{1}{m}$ whether going from $\mathbf{S} \rightarrow \mathbf{S}'$ or $\mathbf{S}' \rightarrow \mathbf{S}$ and will cancel when calculating the acceptance probability, leaving $\prod_{j=1}^h \Pr(S_{d_j} \rightarrow S'_{d_j})$ and $\prod_{j=1}^h \Pr(S'_{d_j} \rightarrow S_{d_j})$.

Case 2 With potential directed cycles there can be multiple paths when moving from the current graph to the proposed graph. Let \mathbf{C}^k be a vector where each c_j^k is the number of edges that can change state in path k when moving from \mathbf{S} to \mathbf{S}' and $\mathbf{C}^{k'}$ be a vector where each $c_j^{k'}$ is the number of edges that can change state in path k when moving from \mathbf{S}' to \mathbf{S} . Using equation (7) the transition probability of moving from the current graph to the proposed graph when there are multiple paths becomes

$$\Pr(\mathbf{S} \rightarrow \mathbf{S}') = \sum_{k=1}^K \prod_{j=1}^h \frac{1}{c_j^k} \prod_{j=1}^h \Pr(S_{d_j} \rightarrow S'_{d_j}) = \prod_{j=1}^h \Pr(S_{d_j} \rightarrow S'_{d_j}) \sum_{k=1}^K \prod_{j=1}^h \frac{1}{c_j^k}.\quad (9)$$

Similarly, the transition probability when there are multiple paths of moving back to the current graph from the proposed graph is

$$\Pr(\mathbf{S}' \rightarrow \mathbf{S}) = \sum_{k=1}^K \prod_{j=1}^h \frac{1}{c_j^{k'}} \prod_{j=1}^h \Pr(S'_{d_j} \rightarrow S_{d_j}) = \prod_{j=1}^h \Pr(S'_{d_j} \rightarrow S_{d_j}) \sum_{k=1}^K \prod_{j=1}^h \frac{1}{c_j^{k'}}.\quad (10)$$

In equations (9) and (10) the summation over K represents the different paths (Section S3) to get from one graph to another and the last equality holds because the edges that are different between \mathbf{S} and \mathbf{S}' do not depend on the path k .

For each path k

$$\mathbf{C}^k = (c_1^k, c_2^k, c_3^k, \dots, c_h^k)\quad (11)$$

$$= (\underbrace{c_1^k, c_2^k, \dots, c_j^k}_{\text{create cycle(s)}}, \underbrace{c_{j+1}^k, \dots, c_h^k}_{\text{remove cycle(s)}})\quad (12)$$

$$= (\underbrace{m, \dots, m}_j, c_{j+1}^k, \dots, c_h^k).\quad (13)$$

The first j elements can create one or more directed cycles. The remaining $h - j$ elements then remove the cycle(s) that were introduced in the network and their values are equal to the number of edges that make up the directed cycle that is being removed. The cycles that are created and removed in any path k from \mathbf{S} to \mathbf{S}' can also be created and removed when moving from \mathbf{S}' to \mathbf{S} . Therefore, the equations for moving from the proposed graph to the current graph will be the same as Equations 11 - 13 except for the ' symbol indicating we are moving backwards:

$$\mathbf{C}^{k'} = (c_1^{k'}, c_2^{k'}, c_3^{k'}, \dots, c_h^{k'}) \quad (14)$$

$$= (\underbrace{c_1^{k'}, c_2^{k'}, \dots, c_j^{k'}}_{\text{create cycle(s)}}, \underbrace{c_{j+1}^{k'}, \dots, c_h^{k'}}_{\text{remove cycle(s)}}) \quad (15)$$

$$= (\underbrace{m, \dots, m}_j, c_{j+1}^{k'}, \dots, c_h^{k'}), \quad (16)$$

and

$$\sum_{k=1}^K \prod_{j=1}^h \frac{1}{c_j^k} = \sum_{k=1}^K \prod_{j=1}^h \frac{1}{c_j^{k'}}. \quad (17)$$

The terms in equation 17 will cancel when calculating the acceptance probability and we will be left with $\prod_{j=1}^h \Pr(S_{d_j} \rightarrow S'_{d_j})$ and $\prod_{j=1}^h \Pr(S'_{d_j} \rightarrow S_{d_j})$. ■

Supplementary figures

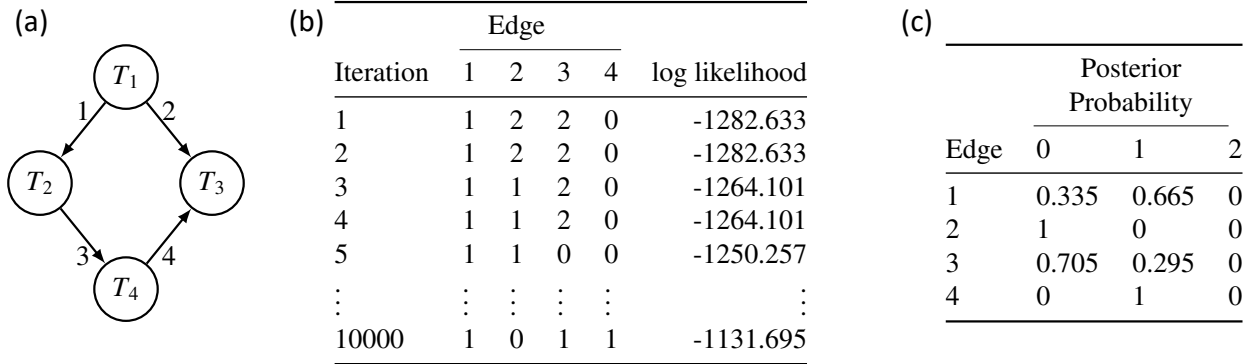


Figure S1: An example of the output from baycn. (a) Topology GN4 (b) Edge states and log likelihood for the graph accepted at each iteration of the Metropolis-Hastings algorithm. (c) The proportion of each edge state provides an estimate of the posterior probability of the edge state for each edge in table (b).

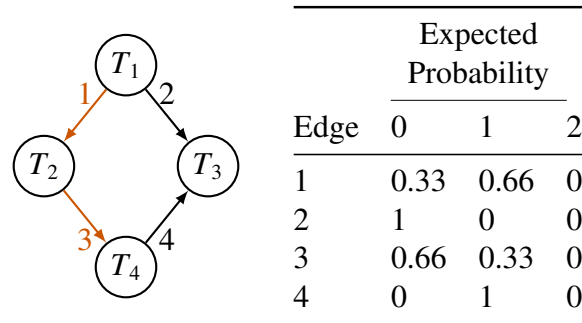


Figure S2: The true graph and expected probabilities for each edge in topology GN4. The edges in orange can change direction while remaining in the Markov equivalence class of the true graph – as long as another v structure is not created.

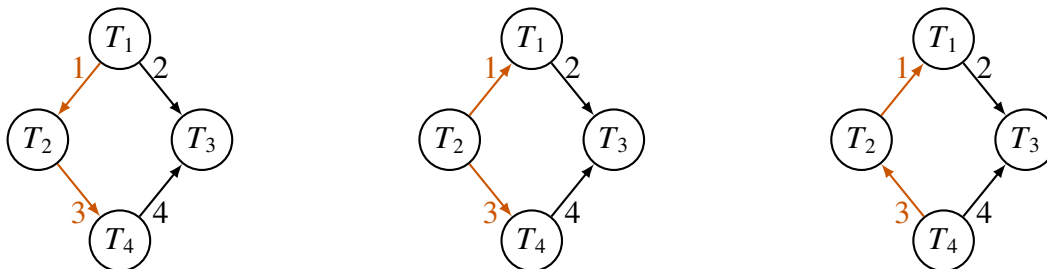
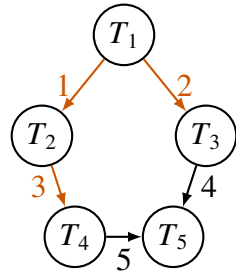


Figure S3: The Markov equivalence class of topology GN4. The edges in orange show all possible combinations of edge directions of the Markov equivalence class. Edge 1 is oriented $T_1 \rightarrow T_2$ in one of the three graphs, giving a proportion of 0.33 for edge state 0. Edge 2 is oriented $T_2 \rightarrow T_4$ in two of the three graphs, giving a proportion of 0.66 for state 0.



Edge	Expected Probability		
	0	1	2
1	0.5	0.5	0
2	0.75	0.25	0
3	0.75	0.25	0
4	1	0	0
5	1	0	0

Figure S4: The true graph and expected probabilities for each edge in topology GN5. The edges in orange can change direction while remaining in the Markov equivalence class of the true graph – as long as another v structure is not created.

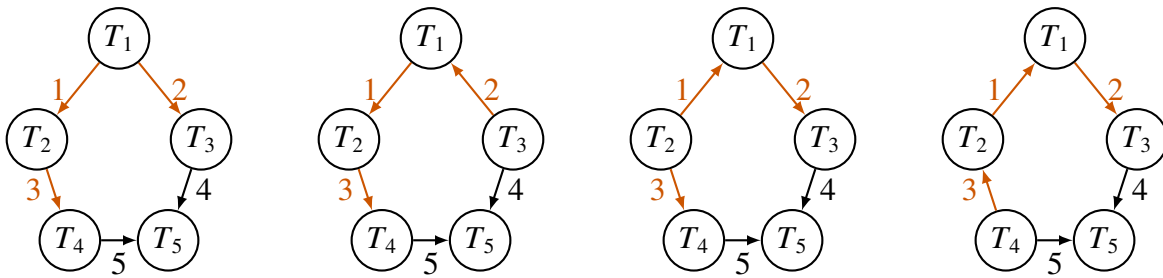
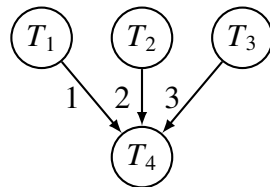


Figure S5: The Markov equivalence class of topology GN5. The edges in orange show all possible combinations of edge directions of the Markov equivalence class. In two of the four graphs edge 1 is oriented $T_1 \rightarrow T_2$, giving a proportion of 0.5 for edge state 0. In three of the four graphs edge 2 is oriented $T_1 \rightarrow T_3$, giving a proportion of 0.75 for edge state 0. Similarly, edge 3 is oriented $T_2 \rightarrow T_4$ in three of the four graphs, giving a proportion of 0.75 for edge state 0.



Edge	Expected Probability		
	0	1	2
1	1	0	0
2	1	0	0
3	1	0	0

Figure S6: The true graph and expected probabilities for each edge in the multi-parent topology.

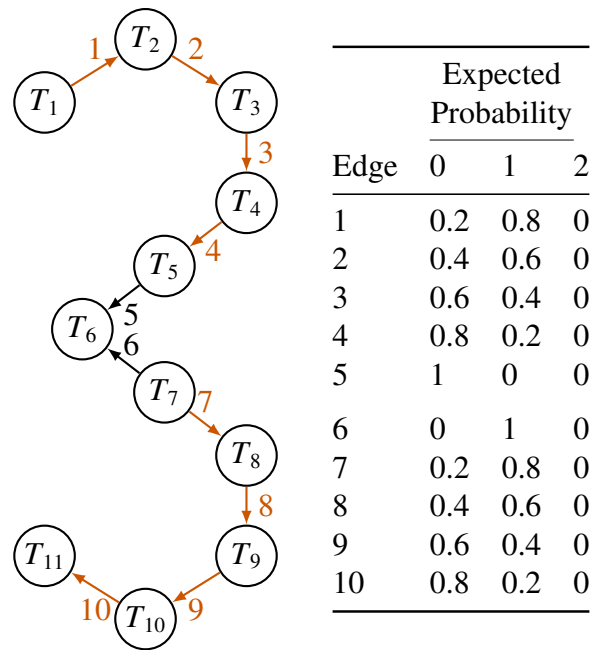


Figure S7: The true graph and expected probabilities for each edge in topology GN11. The edges in orange can change direction while remaining in the Markov equivalence class of the true graph – as long as another v structure is not created.

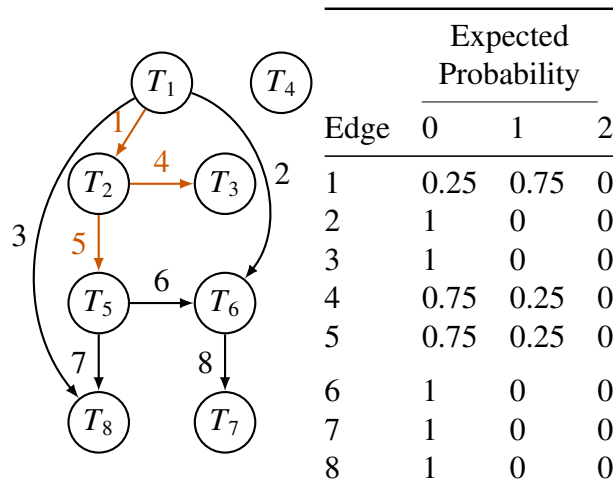


Figure S8: The true graph and expected probabilities for each edge in topology GN8. The edges in orange can change direction while remaining in the Markov equivalence class of the true graph – as long as another v structure is not created.

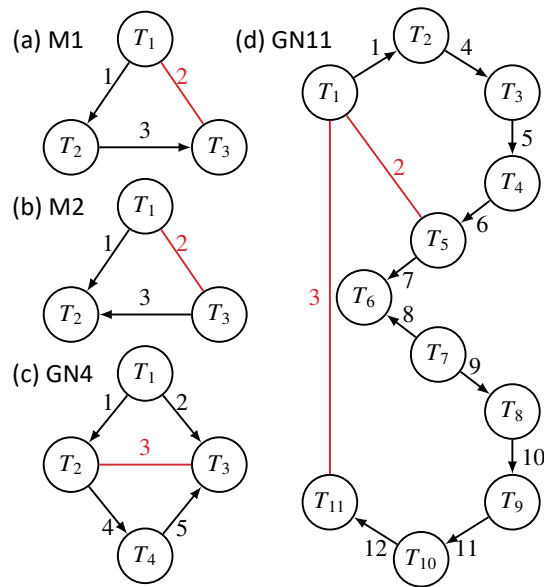


Figure S9: The black edges (true edges) were used to simulate the data and the red edges (false edges) were added to the true adjacency matrix as input to baycn.

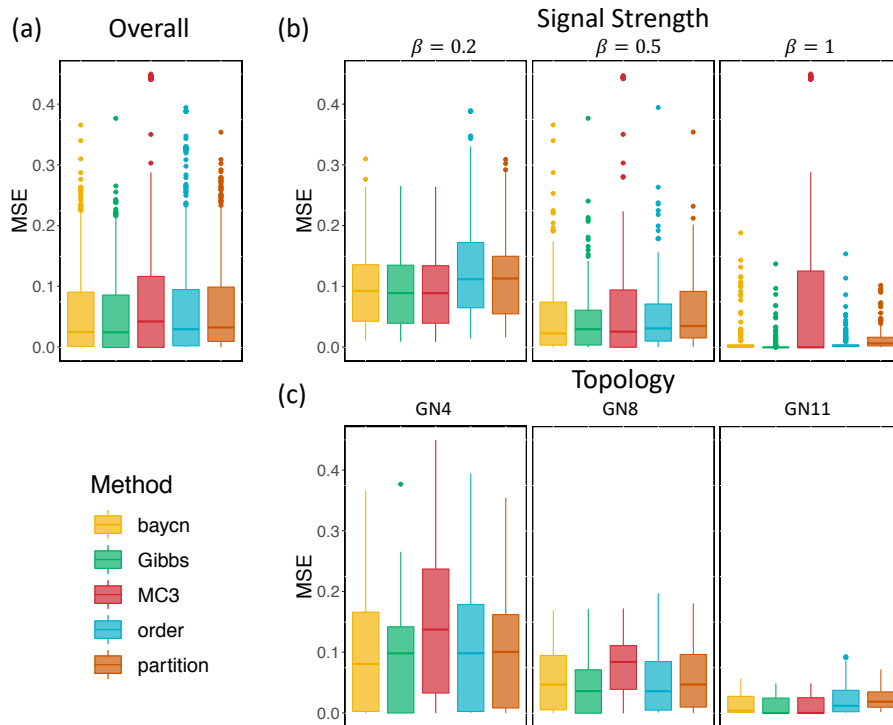


Figure S10: The MSE_3 when the true graph skeleton was the input. (a) MSE grouped by method. (b) MSE grouped by method and β . (c) MSE grouped by method and topology.

Supplementary tables

Table S1: The mean and standard deviation of the edge-wise MSE for each edge in topology M1. We used the data sets previously simulated for M1 and included one false edge with the true edges in the input to baycn. We ran baycn with three different priors on edge states for each data set. The rows in red represent false edges.

		eMSE: Topology M1					
		Prior 1		Prior 2		Prior 3	
N	Edge	mean	sd	mean	sd	mean	sd
100	1	0.0109	0.006	0.0078	0.0047	0.002	0.0026
	2	0.2853	0.0568	0.1859	0.0618	0.0131	0.0139
	3	0.0107	0.0061	0.0091	0.0059	0.0014	0.0015
200	1	0.0116	0.0067	0.0075	0.005	0.002	0.0027
	2	0.2861	0.0816	0.1953	0.0992	0.03	0.0614
	3	0.0109	0.0063	0.0094	0.0046	0.0019	0.0025
600	1	0.0127	0.0062	0.008	0.0056	0.0008	0.001
	2	0.2665	0.038	0.1593	0.052	0.0095	0.0068
	3	0.0139	0.0085	0.0062	0.004	0.0016	0.0021

Table S2: The mean and standard deviation of the edge-wise MSE for each edge in topology M2. We used the data sets previously simulated for M2 and included one false edge with the true edges in the input to baycn. We ran baycn with three different priors on edge states for each data set. The rows in red represent false edges.

		eMSE: Topology M2					
		Prior 1		Prior 2		Prior 3	
N	Edge	mean	sd	mean	sd	mean	sd
100	1	0.1366	0.0269	0.1197	0.0199	0.0224	0.026
	2	0.4035	0.0368	0.3285	0.0548	0.0656	0.0666
	3	0.1461	0.025	0.1241	0.0226	0.0232	0.028
200	1	0.1329	0.0262	0.1215	0.0222	0.0297	0.0354
	2	0.4111	0.0373	0.3474	0.0612	0.0863	0.0975
	3	0.1391	0.0227	0.1209	0.0245	0.0317	0.0396
600	1	0.1369	0.0207	0.1183	0.0221	0.0236	0.0164
	2	0.4062	0.0347	0.3362	0.0459	0.0647	0.0377
	3	0.1378	0.028	0.1186	0.0223	0.0224	0.0149

Table S3: The mean and standard deviation of the edge-wise MSE for each edge in topology GN4. We used the data sets previously simulated for GN4 and included one false edge with the true edges in the input to baycn. We ran baycn with three different priors on edge states for each data set. The rows in red represent false edges.

		eMSE: Topology GN4					
		Prior 1		Prior 2		Prior 3	
N	Edge	mean	sd	mean	sd	mean	sd
100	1	0.0101	0.0182	0.011	0.0165	0.0418	0.0797
	2	0.011	0.0204	0.0098	0.0192	0.0431	0.0821
	3	0.2235	0.1185	0.1368	0.1257	0.0301	0.1031
	4	0.0085	0.0148	0.0078	0.0132	0.0462	0.0817
	5	0.0087	0.0162	0.0107	0.0203	0.0459	0.0888
200	1	0.0012	0.0023	0.0019	0.0036	0.0152	0.0414
	2	0.0004	0.0013	0.0012	0.004	0.0156	0.0462
	3	0.2154	0.079	0.1139	0.0669	0.005	0.0083
	4	0.0013	0.002	0.0023	0.0045	0.0181	0.0432
	5	0.0003	0.001	0.0013	0.0043	0.012	0.0317
600	1	0.0008	0.0015	0.0009	0.001	0.0103	0.0387
	2	0	0	0	0	0.0102	0.0402
	3	0.2534	0.1019	0.1544	0.1028	0.0092	0.0201
	4	0.0007	0.0012	0.0012	0.0015	0.011	0.038
	5	0	0	0	0	0.0112	0.0503

Table S4: The mean and standard deviation of the edge-wise MSE for each edge in topology GN11. We used the data sets previously simulated for GN11 and included two false edges with the true edges in the input to baycn. We ran baycn with three different priors on edge states for each data set. The rows in red represent false edges.

		eMSE: Topology GN11					
N	Edge	Prior 1		Prior 2		Prior 3	
		mean	sd	mean	sd	mean	sd
100	1	0.0023	0.0035	0.003	0.0038	0.0046	0.006
	2	0.2976	0.1311	0.2084	0.1464	0.0386	0.1027
	3	0.2931	0.0658	0.2039	0.0851	0.0168	0.0239
	4	0.0018	0.0028	0.0035	0.0033	0.009	0.0104
	5	0.0029	0.0046	0.0037	0.0048	0.0087	0.0116
	6	0.0045	0.007	0.0043	0.0064	0.0038	0.0044
	7	0	0	0	0	0	0
	8	0	0	0	0	0	0
	9	0.0009	0.0011	0.0014	0.0023	0.0037	0.005
	10	0.0018	0.002	0.002	0.0025	0.0107	0.0153
	11	0.002	0.0019	0.0024	0.0029	0.0097	0.0132
	12	0.0016	0.0018	0.0016	0.0026	0.0044	0.0057
200	1	0.0048	0.0046	0.0033	0.0042	0.0029	0.0036
	2	0.286	0.1233	0.1938	0.1334	0.0338	0.0753
	3	0.3161	0.0676	0.2138	0.0676	0.0188	0.0152
	4	0.0032	0.0052	0.0028	0.0038	0.0076	0.0092
	5	0.0026	0.0043	0.0029	0.006	0.0069	0.0085
	6	0.0041	0.0056	0.0032	0.0056	0.0039	0.0052
	7	0	0	0	0	0	0
	8	0	0	0	0	0	0
	9	0.0006	0.0009	0.0004	0.0005	0.008	0.0137
	10	0.0013	0.0016	0.0007	0.0013	0.0115	0.0148
	11	0.0018	0.0021	0.0014	0.002	0.0093	0.0112
	12	0.0021	0.0025	0.0012	0.0018	0.0038	0.0041
600	1	0.0069	0.0069	0.0052	0.0058	0.0048	0.0056
	2	0.2735	0.0938	0.1783	0.0949	0.0147	0.0231
	3	0.3436	0.1118	0.2446	0.129	0.0557	0.1172
	4	0.0049	0.0062	0.0028	0.003	0.0108	0.0147
	5	0.0024	0.0029	0.0017	0.0021	0.0077	0.0112
	6	0.0027	0.003	0.0015	0.0015	0.0024	0.0023
	7	0	0	0	0	0	0
	8	0	0	0	0	0	0
	9	0.0006	0.0008	0.0009	0.0013	0.0031	0.0036
	10	0.0015	0.0018	0.0023	0.0033	0.0058	0.0069
	11	0.0017	0.0021	0.0029	0.0047	0.0066	0.0087
	12	0.0026	0.005	0.0022	0.0041	0.0046	0.0047

Table S5: The mean and standard deviation of precision, power, and MSE_2 for topology GN4 when a fully connected graph was the input to each algorithm. When calculating precision and power we considered an edge present if the sum of the probability of the two directions was greater than 0.5.

Method	N	β	Precision		Power		MSE_2	
			mean	sd	mean	sd	mean	sd
baycn	100	0.2	0.94	0.2077	0.43	0.2654	0.2398	0.0326
		0.5	0.982	0.0627	0.98	0.0692	0.1235	0.0478
		1	0.9707	0.0841	1	0	0.0439	0.0387
Gibbs	100	0.2	0.942	0.206	0.5	0.2602	0.2163	0.0303
		0.5	0.984	0.0554	1	0	0.1212	0.0299
		1	0.9093	0.1184	1	0	0.0938	0.0592
MC ³	100	0.2	0.942	0.206	0.49	0.265	0.2155	0.0312
		0.5	0.976	0.0663	1	0	0.1215	0.0329
		1	0.9093	0.1184	1	0	0.0945	0.0683
order	100	0.2	0.80	0.4082	0.29	0.2126	0.315	0.0562
		0.5	0.99	0.05	0.96	0.0935	0.1197	0.0502
		1	0.992	0.04	1	0	0.0193	0.0287
partition	100	0.2	0.96	0.2	0.36	0.2051	0.2546	0.04
		0.5	0.982	0.0627	0.98	0.0692	0.1118	0.0357
		1	0.976	0.0663	1	0	0.0287	0.0311
baycn	200	0.2	0.99	0.05	0.74	0.2222	0.1812	0.0427
		0.5	0.992	0.04	1	0	0.101	0.0769
		1	0.984	0.0554	1	0	0.0307	0.0427
Gibbs	200	0.2	0.98	0.0692	0.77	0.2155	0.1763	0.0383
		0.5	0.992	0.04	1	0	0.1134	0.0555
		1	0.952	0.0872	1	0	0.0521	0.0476
MC ³	200	0.2	0.98	0.0692	0.77	0.2155	0.1765	0.0376
		0.5	0.992	0.04	1	0	0.1189	0.0619
		1	0.96	0.0816	1	0	0.0525	0.0452
order	200	0.2	0.9067	0.2809	0.48	0.2385	0.2768	0.0782
		0.5	1	0	1	0	0.1072	0.0721
		1	0.992	0.04	1	0	0.011	0.0349
partition	200	0.2	0.9867	0.0667	0.59	0.2026	0.2087	0.0448
		0.5	0.992	0.04	1	0	0.1043	0.0646
		1	0.992	0.04	1	0	0.012	0.0261
baycn	600	0.2	0.992	0.04	1	0	0.133	0.0358
		0.5	0.992	0.04	1	0	0.0954	0.096
		1	0.992	0.04	1	0	0.0125	0.0102
Gibbs	600	0.2	0.992	0.04	0.99	0.05	0.1274	0.0219
		0.5	0.992	0.04	1	0	0.0982	0.0741
		1	0.992	0.04	1	0	0.0163	0.0156
MC ³	600	0.2	0.992	0.04	0.99	0.05	0.131	0.0225
		0.5	0.992	0.04	1	0	0.1098	0.093
		1	1	0	1	0	0.0153	0.0124
order	600	0.2	1	0	0.96	0.1181	0.1395	0.0391
		0.5	1	0	1	0	0.0909	0.0903
		1	1	0	1	0	0.002	0.0008
partition	600	0.2	1	0	0.97	0.1099	0.1288	0.0272
		0.5	1	0	1	0	0.0869	0.077
		1	1	0	1	0	0.0016	0.0018

Table S6: The mean and standard deviation of MSE_2 when the true skeleton was used as input. We simulated 25 data sets for each combination of topology, N , and β and we ran each algorithm once per data set. MSE_2 is calculated only from the true edges.

Method	N	β	MSE_2					
			GN4		GN8		GN11	
			mean	sd	mean	sd	mean	sd
baycn	100	0.2	0.2305	0.0351	0.2707	0.0294	0.1743	0.0259
		0.5	0.0987	0.0607	0.0951	0.0401	0.0514	0.0322
		1	0.015	0.0414	0.0286	0.0549	0.0064	0.0047
Gibbs	100	0.2	0.2034	0.0292	0.2483	0.0276	0.1504	0.0215
		0.5	0.1009	0.0286	0.0873	0.0242	0.0439	0.03
		1	0.0221	0.0357	0.0313	0.0518	0.0005	0.0003
MC ³	100	0.2	0.2039	0.0279	0.2488	0.0283	0.1508	0.0202
		0.5	0.1022	0.0325	0.0888	0.027	0.0438	0.0299
		1	0.1913	0.2189	0.1573	0.124	0.0003	0.0002
order	100	0.2	0.3144	0.0563	0.368	0.0375	0.271	0.0336
		0.5	0.1187	0.0436	0.0997	0.0384	0.0657	0.0374
		1	0.0146	0.0195	0.0309	0.0432	0.0069	0.0023
partition	100	0.2	0.2505	0.0423	0.316	0.025	0.2067	0.0247
		0.5	0.1125	0.0388	0.1202	0.0478	0.0656	0.0329
		1	0.0213	0.023	0.0393	0.05	0.0291	0.0223
baycn	200	0.2	0.1796	0.0484	0.2129	0.0372	0.1308	0.0269
		0.5	0.1132	0.0958	0.1302	0.0792	0.0182	0.0243
		1	0.0069	0.0214	0.0649	0.1041	0.0098	0.0062
Gibbs	200	0.2	0.1716	0.0487	0.2071	0.0345	0.1239	0.0248
		0.5	0.106	0.0683	0.0871	0.031	0.0134	0.0269
		1	0.0015	0.0052	0.0005	0.0018	0.0004	0.0004
MC ³	200	0.2	0.1725	0.0472	0.2071	0.035	0.1237	0.0252
		0.5	0.1152	0.0966	0.1083	0.0626	0.0133	0.0268
		1	0.2132	0.2264	0.2105	0.1217	0.0003	0.0002
order	200	0.2	0.2743	0.0793	0.2993	0.053	0.2052	0.0459
		0.5	0.1089	0.072	0.0857	0.032	0.0322	0.0327
		1	0.0067	0.0182	0.0051	0.0024	0.0087	0.004
partition	200	0.2	0.2035	0.045	0.2605	0.0325	0.1653	0.0327
		0.5	0.1034	0.0628	0.1136	0.0561	0.0426	0.0259
		1	0.0075	0.0133	0.013	0.0171	0.0327	0.0216
baycn	600	0.2	0.1235	0.0372	0.1721	0.0813	0.0908	0.0288
		0.5	0.0755	0.0903	0.1005	0.0992	0.0071	0.0064
		1	0.0104	0.0273	0.0301	0.0686	0.0068	0.0059
Gibbs	600	0.2	0.125	0.0272	0.1674	0.0724	0.0864	0.0276
		0.5	0.0893	0.0835	0.0651	0.0431	0.0006	0.0012
		1	0	0	0	0	0.0005	0.0004
MC ³	600	0.2	0.1241	0.0282	0.1683	0.0741	0.0868	0.0274
		0.5	0.229	0.2196	0.1316	0.1398	0.0005	0.0013
		1	0.2311	0.2266	0.2232	0.1151	0.0003	0.0002
order	600	0.2	0.1351	0.0397	0.1648	0.069	0.1055	0.0382
		0.5	0.0891	0.0898	0.0518	0.0433	0.0146	0.0158
		1	0.0018	0.0006	0.0038	0.0005	0.0109	0.0052
partition	600	0.2	0.1257	0.028	0.1665	0.0615	0.1	0.0305
		0.5	0.091	0.0803	0.0736	0.0792	0.0394	0.02
		1	0.001	0.0015	0.0059	0.0146	0.0477	0.0389

Table S7: The mean and standard deviation of the MSE_3 when the true skeleton was used as input. We simulated 25 data sets for each combination of topology, N , and β and we ran each algorithm once per data set. MSE_3 is calculated from all possible edges in the network.

Method	N	β	MSE_3					
			GN4		GN8		GN11	
			mean	sd	mean	sd	mean	sd
baycn	100	0.2	0.1537	0.0234	0.0773	0.0084	0.0317	0.0047
		0.5	0.0658	0.0404	0.0272	0.0115	0.0094	0.0059
		1	0.01	0.0276	0.0082	0.0157	0.0012	0.0008
Gibbs	100	0.2	0.1356	0.0195	0.0709	0.0079	0.0273	0.0039
		0.5	0.0673	0.0191	0.0249	0.0069	0.008	0.0055
		1	0.0147	0.0238	0.0089	0.0148	0.0001	0.0001
MC ³	100	0.2	0.1359	0.0186	0.0711	0.0081	0.0274	0.0037
		0.5	0.0681	0.0217	0.0254	0.0077	0.008	0.0054
		1	0.1276	0.1459	0.0449	0.0354	0	0
order	100	0.2	0.2097	0.0375	0.1088	0.0124	0.051	0.007
		0.5	0.081	0.0318	0.0302	0.0124	0.0138	0.0083
		1	0.0125	0.0184	0.0126	0.0129	0.002	0.0017
partition	100	0.2	0.169	0.0277	0.0949	0.0095	0.0404	0.005
		0.5	0.0778	0.0279	0.0381	0.0152	0.0149	0.007
		1	0.0186	0.0195	0.0158	0.0149	0.0073	0.004
baycn	200	0.2	0.1197	0.0323	0.0608	0.0106	0.0238	0.0049
		0.5	0.0755	0.0639	0.0372	0.0226	0.0033	0.0044
		1	0.0046	0.0142	0.0185	0.0297	0.0018	0.0011
Gibbs	200	0.2	0.1144	0.0325	0.0592	0.0098	0.0225	0.0045
		0.5	0.0707	0.0455	0.0249	0.0089	0.0024	0.0049
		1	0.001	0.0035	0.0001	0.0005	0.0001	0.0001
MC ³	200	0.2	0.115	0.0315	0.0592	0.01	0.0225	0.0046
		0.5	0.0768	0.0644	0.0309	0.0179	0.0024	0.0049
		1	0.1421	0.151	0.0601	0.0348	0.0001	0
order	200	0.2	0.1846	0.0527	0.0878	0.016	0.0381	0.0086
		0.5	0.0727	0.0479	0.0257	0.0105	0.008	0.0073
		1	0.0068	0.0204	0.0026	0.0039	0.003	0.0031
partition	200	0.2	0.1377	0.0305	0.077	0.0089	0.0318	0.0064
		0.5	0.0697	0.0414	0.0347	0.0174	0.0106	0.0059
		1	0.0075	0.0142	0.0064	0.0059	0.0078	0.0046
baycn	600	0.2	0.0824	0.0248	0.0492	0.0232	0.0165	0.0052
		0.5	0.0503	0.0602	0.0287	0.0283	0.0013	0.0012
		1	0.0069	0.0182	0.0086	0.0196	0.0012	0.0011
Gibbs	600	0.2	0.0834	0.0181	0.0478	0.0207	0.0157	0.005
		0.5	0.0595	0.0557	0.0186	0.0123	0.0001	0.0002
		1	0	0	0	0	0.0001	0.0001
MC ³	600	0.2	0.0828	0.0188	0.0481	0.0212	0.0158	0.005
		0.5	0.1527	0.1464	0.0376	0.0399	0.0001	0.0002
		1	0.1541	0.1511	0.0638	0.0329	0.0001	0
order	600	0.2	0.0902	0.0266	0.048	0.0193	0.0201	0.0071
		0.5	0.0595	0.0597	0.0162	0.0136	0.0034	0.0041
		1	0.0013	0.0005	0.0019	0.0035	0.003	0.0026
partition	600	0.2	0.0843	0.0189	0.0488	0.0173	0.0198	0.0055
		0.5	0.0611	0.0534	0.0225	0.0229	0.0087	0.0041
		1	0.0012	0.0016	0.0033	0.0054	0.0102	0.0076

Table S8: The mean runtime in seconds across 25 data sets. For each topology 25 data sets were generated with $\beta = 1$ and $N = 600$ and each algorithm was run once per data set and the runtime in seconds was recorded. All algorithms were run on an Intel Xeon D-1540 2.00 GHz processor with 128 GB of memory.

Topology	Runtime				
	baycn	Gibbs	MC ³	order	partition
GN4	4.49	235.00	11.94	1.78	3.93
GN8	8.11	363.91	22.49	2.88	7.97
GN11	7.07	380.97	23.52	3.10	9.39

Table S9: The posterior probability of the three edge states for baycn and partition MCMC from the first 7 simulated data sets of GN4 (Figure S2) with $N = 100$ and $\beta = 0.2$. The edges in red are the false edges, edge numbers with -v are the edges that make a v structure, and the edge numbers in bold are the edges where baycn inferred a true edge as present but partition MCMC did not.

		GN4: Fully connected graph					
		baycn			partition		
data set	Edge	0	1	2	0	1	2
1	1	0.08	0.045	0.875	0.032	0.04	0.928
	2-v	0.12	0.085	0.795	0.045	0.047	0.908
	3	0.025	0.055	0.92	0.03	0.026	0.944
	4	0.08	0.045	0.875	0.044	0.029	0.928
	5	0.265	0.21	0.525	0.173	0.117	0.709
	6-v	0.48	0.515	0.005	0.536	0.463	0.001
2	1	0.435	0.405	0.16	0.405	0.358	0.237
	2-v	0.045	0.075	0.88	0.025	0.027	0.948
	3	0.035	0.1	0.865	0.025	0.04	0.935
	4	0.245	0.32	0.435	0.209	0.289	0.501
	5	0.2	0.36	0.44	0.145	0.244	0.611
	6-v	0.505	0.44	0.055	0.516	0.434	0.05
3	1	0.515	0.385	0.1	0.473	0.349	0.178
	2-v	0.285	0.285	0.43	0.177	0.226	0.597
	3	0.19	0.34	0.47	0.161	0.213	0.626
	4	0.085	0.045	0.87	0.039	0.037	0.924
	5	0.25	0.435	0.315	0.204	0.363	0.433
	6-v	0.15	0.25	0.6	0.126	0.133	0.741
4	1	0.14	0.105	0.755	0.101	0.097	0.802
	2-v	0.185	0.19	0.625	0.126	0.132	0.742
	3	0.055	0.095	0.85	0.051	0.081	0.868
	4	0.085	0.06	0.855	0.056	0.047	0.897
	5	0.455	0.54	0.005	0.511	0.488	0.001
	6-v	0.185	0.18	0.635	0.105	0.121	0.774
5	1	0.16	0.175	0.665	0.142	0.152	0.706
	2-v	0.175	0.115	0.71	0.076	0.06	0.864
	3	0.09	0.09	0.82	0.047	0.031	0.921
	4	0.06	0.095	0.845	0.025	0.026	0.949
	5	0.075	0.06	0.865	0.036	0.052	0.911
	6-v	0.485	0.46	0.055	0.499	0.464	0.037
6	1	0.165	0.25	0.585	0.153	0.132	0.714
	2-v	0.52	0.475	0.005	0.469	0.491	0.04
	3	0.045	0.08	0.875	0.032	0.04	0.928
	4	0.03	0.025	0.945	0.03	0.029	0.941
	5	0.1	0.125	0.775	0.066	0.057	0.877
	6-v	0.06	0.035	0.905	0.036	0.022	0.941
7	1	0.48	0.43	0.09	0.416	0.383	0.201
	2-v	0.065	0.085	0.85	0.05	0.045	0.905
	3	0.05	0.05	0.9	0.039	0.06	0.901
	4	0.11	0.04	0.85	0.059	0.024	0.918
	5	0.145	0.18	0.675	0.097	0.117	0.786
	6-v	0.16	0.2	0.64	0.13	0.116	0.754

Table S10: The posterior probability of the three edge states for baycn and partition MCMC from the first 7 simulated data sets of GN4 (Figure S2) with $N = 200$ and $\beta = 0.2$. The edges in red are the false edges, edge numbers with -v are the edges that make a v structure, and the edge numbers in bold are the edges where baycn inferred a true edge as present but partition MCMC did not.

		GN4: Fully connected graph					
		baycn			partition		
data set	Edge	0	1	2	0	1	2
1	1	0.415	0.38	0.205	0.389	0.257	0.354
	2-v	0.425	0.515	0.06	0.419	0.459	0.122
	3	0.095	0.045	0.86	0.037	0.032	0.93
	4	0.075	0.09	0.835	0.037	0.054	0.909
	5	0.14	0.115	0.745	0.056	0.091	0.853
	6-v	0.605	0.395	0	0.599	0.392	0.01
2	1	0.33	0.67	0	0.272	0.728	0
	2-v	0.335	0.645	0.02	0.231	0.692	0.077
	3	0.03	0.075	0.895	0.015	0.031	0.954
	4	0.23	0.16	0.61	0.121	0.079	0.8
	5	0.37	0.34	0.29	0.204	0.172	0.623
	6-v	0.525	0.475	0	0.475	0.509	0.016
3	1	0.37	0.385	0.245	0.298	0.294	0.408
	2-v	0.32	0.285	0.395	0.218	0.19	0.592
	3	0.025	0.07	0.905	0.02	0.016	0.964
	4	0.13	0.085	0.785	0.072	0.065	0.863
	5	0.335	0.535	0.13	0.349	0.43	0.221
	6-v	0.32	0.44	0.24	0.253	0.286	0.461
4	1	0.11	0.13	0.76	0.07	0.051	0.879
	2-v	0.415	0.29	0.295	0.3	0.181	0.519
	3	0.135	0.07	0.795	0.052	0.046	0.901
	4	0.115	0.19	0.695	0.076	0.125	0.799
	5	0.235	0.25	0.515	0.141	0.188	0.671
	6-v	0.385	0.525	0.09	0.378	0.461	0.161
5	1	0.51	0.48	0.01	0.498	0.47	0.032
	2-v	0.41	0.4	0.19	0.383	0.312	0.305
	3	0.035	0.045	0.92	0.019	0.021	0.96
	4	0.045	0.035	0.92	0.016	0.021	0.963
	5	0.505	0.485	0.01	0.484	0.494	0.022
	6-v	0.335	0.385	0.28	0.231	0.304	0.465
6	1	0.225	0.17	0.605	0.146	0.103	0.751
	2-v	0.56	0.44	0	0.591	0.403	0.006
	3	0.4	0.48	0.12	0.47	0.367	0.163
	4	0.03	0.05	0.92	0.021	0.02	0.959
	5	0.34	0.605	0.055	0.31	0.562	0.127
	6-v	0.285	0.295	0.42	0.17	0.19	0.641
7	1	0.335	0.36	0.305	0.248	0.233	0.519
	2-v	0.27	0.235	0.495	0.166	0.157	0.677
	3	0.075	0.035	0.89	0.02	0.019	0.961
	4	0.105	0.12	0.775	0.059	0.082	0.859
	5	0.325	0.46	0.215	0.234	0.406	0.359
	6-v	0.425	0.575	0	0.439	0.546	0.015

Table S11: The posterior probability of the three edge states for baycn and partition MCMC from the first 7 simulated data sets of GN4 (Figure S2) with $N = 600$ and $\beta = 0.2$. The edges in red are the false edges, edge numbers with -v are the edges that make a v structure, and the edge numbers in bold are the edges where baycn inferred a true edge as present but partition MCMC did not.

		GN4: Fully connected graph					
		baycn			partition		
data set	Edge	0	1	2	0	1	2
1	1	0.61	0.39	0	0.511	0.489	0
	2-v	0.345	0.325	0.33	0.224	0.148	0.627
	3	0.065	0.03	0.905	0.02	0.012	0.968
	4	0.065	0.045	0.89	0.016	0.016	0.968
	5	0.405	0.595	0	0.491	0.509	0
	6-v	0.29	0.26	0.45	0.091	0.142	0.767
2	1	0.61	0.39	0	0.632	0.368	0
	2-v	0.585	0.415	0	0.641	0.359	0
	3	0.025	0.055	0.92	0.009	0.014	0.978
	4	0.05	0.05	0.9	0.017	0.014	0.969
	5	0.36	0.64	0	0.424	0.576	0
	6-v	0.445	0.555	0	0.401	0.589	0.01
3	1	0.63	0.37	0	0.615	0.385	0
	2-v	0.465	0.465	0.07	0.379	0.384	0.237
	3	0.13	0.095	0.775	0.037	0.034	0.929
	4	0.095	0.15	0.755	0.019	0.03	0.951
	5	0.44	0.56	0	0.426	0.574	0
	6-v	0.645	0.355	0	0.54	0.46	0
4	1	0.57	0.43	0	0.469	0.53	0.001
	2-v	0.555	0.39	0.055	0.368	0.431	0.201
	3	0.065	0.065	0.87	0.007	0.01	0.983
	4	0.085	0.055	0.86	0.007	0.01	0.983
	5	0.63	0.37	0	0.505	0.495	0
	6-v	0.45	0.55	0	0.495	0.505	0
5	1	0.545	0.455	0	0.586	0.414	0
	2-v	0.515	0.485	0	0.602	0.392	0.006
	3	0.025	0.045	0.93	0.007	0.006	0.986
	4	0.065	0.04	0.895	0.012	0.01	0.978
	5	0.525	0.475	0	0.439	0.559	0.002
	6-v	0.355	0.645	0	0.425	0.575	0
6	1	0.765	0.23	0.005	0.758	0.233	0.009
	2-v	0.645	0.355	0	0.682	0.314	0.004
	3	0.15	0.07	0.78	0.02	0.015	0.965
	4	0.06	0.05	0.89	0.007	0.006	0.986
	5	0.33	0.67	0	0.232	0.768	0
	6-v	0.375	0.625	0	0.283	0.711	0.006
7	1	0.425	0.575	0	0.46	0.54	0
	2-v	0.4	0.6	0	0.5	0.5	0
	3	0.055	0.06	0.885	0.006	0.012	0.981
	4	0.06	0.06	0.88	0.012	0.017	0.97
	5	0.5	0.5	0	0.569	0.431	0
	6-v	0.45	0.55	0	0.534	0.46	0.006

References

- Badsha, M. B., and Fu, A. Q. (2019), “Learning causal biological networks with the principle of Mendelian randomization,” *Frontiers in Genetics*, 10.
- Badsha, M. B., Martin, E. A.— (2018), “MRPC: An R package for accurate inference of causal graphs,” *arXiv preprint arXiv:1806.01899*.
- Colombo, D., and Maathuis, M. H. (2014), “Order-independent constraint-based causal structure learning,” *The Journal of Machine Learning Research*, 15, 3741–3782.
- Friedman, N., and Koller, D. (2003), “Being Bayesian about network structure. A Bayesian approach to structure discovery in Bayesian networks,” *Machine Learning*, 50, 95–125.
- Giudici, P., and Castelo, R. (2003), “Improving Markov chain Monte Carlo model search for data mining,” *Machine Learning*, 50, 127–158.
- Goudie, R. J., and Mukherjee, S. (2016), “A Gibbs sampler for learning DAGs,” *The Journal of Machine Learning Research*, 17, 1032–1070.
- Grzegorzczak, M., and Husmeier, D. (2008), “Improving the structure MCMC sampler for Bayesian networks by introducing a new edge reversal move,” *Machine Learning*, 71, 265.
- He, Y., Jia, J., Yu, B. et al. (2013), “Reversible MCMC on Markov equivalence classes of sparse directed acyclic graphs,” *The Annals of Statistics*, 41, 1742–1779.
- Kalisch, M., Mächler, M., Colombo, D., Maathuis, M. H., Bühlmann, P. et al. (2012), “Causal inference using graphical models with the R package pcalg,” *Journal of Statistical Software*, 47, 1–26.
- Koller, D., and Friedman, N. (2009), *Probabilistic Graphical Models: Principles and Techniques*, MIT Press.
- Korb, K. B., and Nicholson, A. E. (2010), *Bayesian Artificial Intelligence*, CRC Press.
- Kuipers, J., and Moffa, G. (2017), “Partition MCMC for inference on acyclic digraphs,” *Journal of the American Statistical Association*, 112, 282–299.
- Kuipers, J., Suter, P.— (2018), “Efficient Structure Learning and Sampling of Bayesian Networks,” *arXiv preprint arXiv:1803.07859*.
- Leday, G. G., and Richardson, S. (2018), “Fast Bayesian inference in large Gaussian graphical models,” *arXiv preprint arXiv:1803.08155*.
- Madigan, D., York, J., and Allard, D. (1995), “Bayesian graphical models for discrete data,” *International Statistical Review/Revue Internationale de Statistique*, 63, 215–232.
- Margaritis, D. (2003), “Learning Bayesian Network Model Structure from Data,” Ph.D. thesis, School of Computer Science, Carnegie-Mellon University, Pittsburgh, PA, available as Technical Report CMU-CS-03-153.
- Mohammadi, A., Wit, E. C. et al. (2015), “Bayesian structure learning in sparse Gaussian graphical models,” *Bayesian Analysis*, 10, 109–138.

- Russell, S. J., and Norvig, P. (2009), *Artificial Intelligence: A Modern Approach*, Prentice Hall.
- Schwaller, L., Robin, S., and Stumpf, M. (2015), “A closed-form approach to Bayesian inference in tree-structured graphical models,” *arXiv preprint arXiv:1504.02723*.
- Scutari, M. (2009), “Learning Bayesian networks with the bnlearn R package,” *arXiv preprint arXiv:0908.3817*.
- Spirtes, P., Glymour, C. N., and Scheines, R. (2000), *Causation, Prediction, and Search*, MIT Press.
- Tsamardinos, I., Brown, L. E., and Aliferis, C. F. (2006), “The max-min hill-climbing Bayesian network structure learning algorithm,” *Machine Learning*, 65, 31–78.
- Verma, T., and Pearl, J. (1990), “Equivalence and synthesis of causal models,” in *Proceedings of the Sixth Annual Conference on Uncertainty in Artificial Intelligence*, Elsevier Science Inc., pp. 255–270.